Dynamic Modeling of AFM Cantilever Probe Under Base Excitation system

Mr. Manojkumar Madhukar Salgar

Department of Mechanical Engineering
National Institute of technology, Rourkela
Rourkela – 769008, Odhisha, INDIA

June 2013

Dynamic Modeling of AFM Cantilever Probe Under Base Excitation system

A thesis submitted in partial fulfillment of the
requirements for the degree of

Master of Technology

in

Machine Design and Analysis

by

Mr. Manojkumar Madhukar Salgar
(Roll no: 211ME1155)
Salgar.manoj@gmail.com

Under the guidance of
Dr. (Prof.) J. Srinivas

Department of Mechanical Engineering
National Institute of technology, Rourkela
Rourkela – 769008, Odhisha, INDIA

2011-2013

Department of Mechanical Engineering
National Institute of Technology, Rourkela

C E R T I F I C A T E

*This is to certify that the thesis entitled "**Dynamic Modeling of AFM Cantilever Probe Under Base Excitation system**" by **Mr. Manojkumar Madhukar Salgar,** submitted to the National Institute of Technology, Rourkela for the award of Master of Technology in **Mechanical engineering** with the specialization of **"Machine Design and Analysis"**, is a record of bonafide research work carried out by him in the **Department of Mechanical Engineering**, under my supervision and guidance. I believe that this thesis fulfills part of the requirements for the award of the degree of Master of Technology. The results embodied in this thesis have not been submitted for the award of any other degree elsewhere.*

Dr. (Prof.) J. Srinivas
Department of Mechanical Engineering
National Institute of Technology
Rourkela – 769008, Odisha,
INDIA

Place: N.I.T., Rourkela
Date :

Acknowledgement

First and foremost, I am truly indebted to my supervisor professor J. Srinivas for his guidance, inspiration and showing confidence in me, without which this thesis would not be in its present form. I also thank him for his encoraging words and teaching me a way to look at things very differently.

I express my gratitude to the professors of my specialization, professor S. C. Mohanty for their advice and care. I am also very much obliged to the Head of the Department of Mechanical Engineering Prof K. P. Maity. NIT Rourkela for providing all the possible facilities towards this work. Also thanks to other faculty members in the department.

I would like to thank Mr. Prasad Inamdar, Mr. Prabhu L (PhD Scholar) and Varalakshmi madam at NIT Rourkela, for their enjoyable and helpful company.

My whole hearted gratitude to my parents, Sharada and Madhukar Salgar and my brother Mukund for their encouragement and support.

Manojkumar Madhukar Salgar
Rourkela, June 2013

ABSTRACT

Atomic force microscopy (AFM) can be used for atomic and nanoscale surface characterization in both air and liquid environments. AFM is basically used to measure the mechanical, chemical and biological properties of the sample under investigation. AFM contains basically a base-excited microcantilever with nano tip along with a sensing circuit for scanning of images. Design and analysis of this microcantilevers is a challenging task in real time practice. In the present work, design and dynamic analysis of rectangular microcantilevers in tapping mode with tip-mass effect is considered. Computer simulations are performed with both lumped-parameter and distributed parameter models. The interatomic forces between the nano tip mass and substrate surfaces are treated using Lennard Jones (LJ) model and DMT model. The equations of motion are derived for both one-degree of freedom lumped parameter model with squeeze-film damping and distributed parameter model under the harmonic base excitation. Also the nonlinearity of the cantilever is investigated by considering cubic stiffness. The distributed parameter model is simplified with one mode approximation using Galerkin's scheme. The resulting nonlinear dynamic equations are solved using in numerical Runge-Kutta method using a MATLAB program. The natural frequencies of the microcantilever and dynamic response are obtained. Dynamic stability issues are studied using phase diagrams and frequency responses. An experimental work is carried out to understand the variations in dynamic characteristics of a chromium plated steel microcantilever specimen fabricated using wire-cut EDM process. An electrodynamic exciter is attached at the cantilever base and laser Doppler Vibrometer (LDV) is used to provide sensing signal at the oscilloscope. The sine sweep excitation is provided by a signal generator and power amplifier set-up. The frequency response obtained manually is used to arrive-at the natural frequencies and damping factors.

The principle of atomic force microscope can be used in micro sensing applications in many areas like aerospace, biological and fluid-flow engineering. The microsensor in such applications encounters various types of fluid media. Therefore, the study of conventional micro-cantilevers is not applicable in liquids. The behavior of the AFM cantilever in liquid media has been studied by many researchers during the past five years. Hydrodynamic forces in the system are often modeled as nonlinear functions of the tip displacement. On the other hand micro-cantilevers sensors can also be used for measurement of microscale viscosity, density, and temperature in avionic applications by analyzing the frequency response of the cantilever. In this line, present work considers the additional hydrodynamic forces in the model equations of base-excited cantilever system with its tip operating in tapping mode. The results of the one-mode approximated distributed parameter model are tried to validate with finite element model of the beam operating in liquids.

Index

NOMENCLATURE

L	Length of microcantilever beam
b	Width of microcantilever beam
t	Thickness of microcantilever beam
z_0	Equilibrium gap between microcantilever tip and sample
R	Equivalent radius of the tip
A_1, A_2	Hamarker's constants
η	Kinematic viscosity
m_e	Equivalent tip mass
l	Tip length
Q	Quality factor
k	Bending stiffness of microcantilever
E	Young's modulus of microcantilever
ρ	Density of microcantilever
μ	Poisson's ratio
ω	Natural frequency
μ_{eff}	Effective dynamic viscosity
ϕ	Mode shape function
a_0	intermolecular distance
ρ_{liq}	Density of fluid
E^*	Effective elastic modulus
G^*	Effective elastic modulus
M	Global mass matrix
C	Global damping matrix
K	Global stiffness matrix

LIST OF FIGURES

LIST OF TABLES

CHAPTER 1

1. INTRODUCTION

Scanning probe microscope (SPM) is an instrument used to image and measure properties of material, chemical and biological surfaces. SPM images are obtained by scanning a sharp probe across the surface using tip-sample interactions to get an image. There two basic forms of SPM are scanning tunneling microscopy (STM) and Atomic Force Microscopy (AFM). The STM was first developed in 1982 at IBM in Zurich by Binning et al.

The scanning tunneling microscope is used to measure force at the atomic levels. The atomic force microscope is a combination of a scanning tunneling microscope and the stylus. Invented in year 1985, the AFM has become one of the most versatile instrument in nanotechnology. AFM operates in a much similar way as a blind person reads a book. However, instead of moving a hypersensitive fingertip over the Braille language, the AFM moves its tiny probing finger over much smaller objects such as DNA molecules, live yeast cells or the atomic plateaus on a graphite surface. The AFM finger is actually, a cantilever beam about a few hundred micrometers long, with a very sharp pointed tip protruding off the bottom, similar to the needle of a record player. This probe is scanned back and forth across a specimen. The best resolution reported for AFM is of order 0.01 nm measured in vacuum, but AFM can be used in air and in liquids.

Atomic force microscope consists of a tip mounted on a microcantilever and is close to the specimen surface as shown in Fig.1.1. Most of the cases cantilever is made up of silicon or silicon nitride with tip radius of curvature in orders of nanometers. As the tip moves on the surface to be investigated, the forces like van der Waals' forces, capillary forces, chemical bonding, electrostatic forces, magnetic forces etc. between the tip and the surface induces the transverse displacement of the tip. The cantilever motion can either be measured optically or by using sensing elements built into the cantilever itself. In optical approach, a laser beam is

transmitted to the tip of the cantilever and allowed to reflect back. The reflected laser beam is detected using a photosensitive detector located few centimeters away.

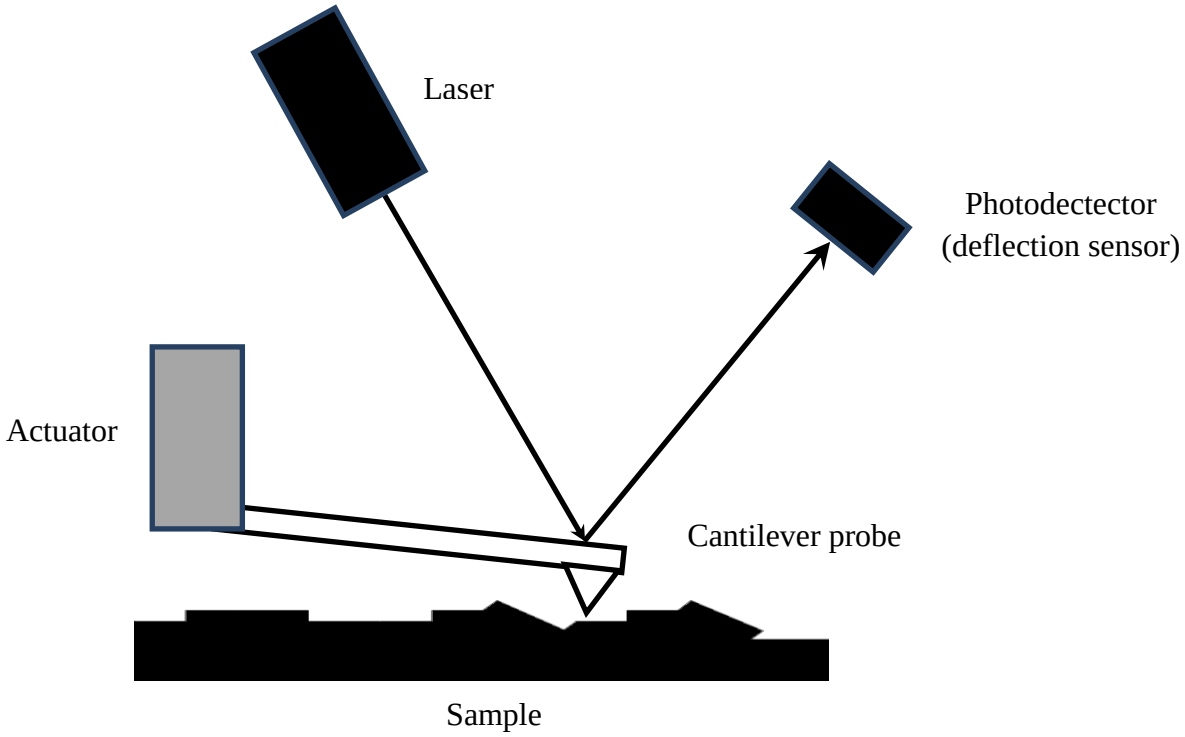

Fig.1.1 AFM Schematic Diagram with microcantilever

The output of this photosensitive detector is provided to the computer for processing the data so that we can get a topographical image of the surface with atomic resolution. Atomic force microscopy is used to measure the forces as small as 10^{-18}N.

There are three basic operating modes of AFM: (i) contact mode, (ii) noncontact mode, and (iii) tapping mode. In contact mode, the tip of the cantilever is always in contact with the sample surface. The cantilever beam acts as a spring, so the tip is always pushing very lightly against the sample. In this mode, overall forces are repulsive. As the probe encounters surface features, the microscope adjusts the vertical position of the cantilever's base so that force applied to the sample remains constant. This is done in a feedback loop. In noncontact mode (1987), tip of the cantilever does not in contact with the sample surface. Nonetheless, in noncontact mode, the probe needs to be excited at or near its resonant frequency, while the

distance between the tip and sample's surface must be kept constant. In tapping mode (1993), cantilever oscillates up and down near to its resonance frequency. That is, the probe's tip can hover over the sample's surface while the microcantilever is oscillating at amplitudes mainly higher than the amplitudes in the noncontact mode. The amplitude of oscillation is typically 20-100nm. The amplitude of oscillation decreases when the probe's tip approaches the surface due to nanoscale interaction forces. This mode is well suited to examine soft (biological) samples that are too fragile for the lateral, dragging force exerted in contact mode. In tapping mode, the feedback loop does not have a set point deflection to maintain; it strives to maintain a set point amplitude. In the tapping mode, cantilever may either have a frequency modulation (FM) mode or amplitude modulation mode. In FM mode, cantilever is made to oscillates at its natural frequency and when it is brought close to the sample, the long range forces between the tip and sample cause the frequency to shift. Thus, feedback loop works to maintain a set point frequency. This keeps the tip-sample distance constant so that surface topography can be measured.

Being the main part of AFM, microcantilever probe system requires close attention. Accurate simulation of cantilever dynamics coupled with nonlinear tip-sample interactions necessitates the comprehensive techniques during the modeling.

1.1 MICROCANTILEVER OF ATOMIC FORCE MICROSCOPY

Microcantilever is the basic element of Atomic Force Microscope. It is used to get information on shape and dimensions of the element that is being studied. Fig. 1.2 shows the schematic diagram of a V-shaped AFM cantilever. The cantilever is placed just above the sample specimen, which is under investigation. This cantilever moves over a sample specimen surface and due to the attractive and repulsive forces, it starts to vibrate. Up till now the designs of microcantilever of atomic force microscope are divided in to two groups. In

first group there are micro-probes with tip in the form of a cone or pyramid. Scanning across a surface, AFM interacts with the sample surface through its tip.

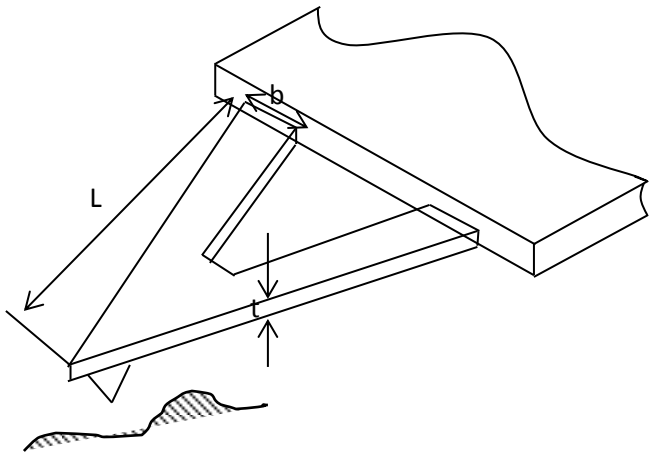

Fig.1.2 Typical V-Shaped microcantilever beam

According to the nonlinear nature of the tip-sample interaction forces, the behavior of the cantilever is nonlinear. The imaging rate and contrast of topographical images considerably depends on the resonant frequency and sensitivity of the cantilever. Therefore, an accurate model to represent the mechanics of microcantilever is very much important in order to study the AFM system and improve the resolution of the acquired image. There are several models available in literature such as lumped-parameter models and distributed parameter models. In lumped-parameter models, the lower frequency oscillations are utilized when first few modes are excited. To represent a distributed parameter model of an AFM cantilever using Euler-Bernoulli beam theory, there are advanced models in literature. For small beams, the Timoshenko beam assumptions are required where the shear deformation and rotary inertia becomes significant. Different tip-sample interaction force assumptions are also available. These forces can be expressed either in the form of Hertz contact model, piecewise linear contact model, Derjaguin-Muller-Toporov (DMT), a combination of the van der Waals attraction and the electrostatic repulsion between two surfaces in a liquid environment etc. These microcantilever structures are often made-up of silicon/silicon nitrides.

1.2 LITERATURE SURVEY

This section deals with relevant literature available on the dynamics and control of AFM cantilevers. Several authors dealt with design issues with reference to various configurations of cantilevers such as triangular and rectangular tapered cantilevers.

1.2.1 Design Issues

G. Binning et al. [1] and A. Raman et al. [2] proposed a system where the scanning tunneling microscope (STM) is used to measure the motion of cantilever beam with an ultra-small mass and designed a new tool atomic force microscope (AFM) to increase level of sensitivity. AFM is used to measure any type of force; not only interatomic forces, but electromagnetic forces as well.

Zhang et al. [3] presented nonlinear dynamics and chaos of a tip-sample dynamic system in tapping mode by modelling microcantilever as a spring-mass system and interaction force was considered as Lennard Jones (LJ) potential.

Payam and Fathipour [4] presented dynamic mode AFM microcantilever-tip system based on Euler's beam theory and solved it numerically to study the effects of tip mass, beam density, length and interaction forces by linearizing all the terms.

Korayem et al. [5] studied the dynamic behavior of microcantilever-sample system in tapping mode and adopted the sliding mode controller design for minimizing the nonlinear behavior.

Brenetto et al. [6] explored the possibilities of extracting energy from mechanical vibration using ionic polymer metal composites in which the hydrodynamic function-expressions were proposed over some range of Reynolds's numbers.

Lee et al. [7] proposed an improved theoretical approach to predict dynamic behavior of long, slender and flexible microcantilevers affected by squeeze film damping at low

ambient pressure. They investigated the relative importance of theoretical assumption made in the Reynolds-equation-based approach for flexible micro electromechanical systems. The uncertainties in damping ratio prediction introduced due to assumption to the gas refraction effect, gap height and pressure boundary conditions are studied. They attempted to calculate squeeze film damping ratios of higher order bending modes of flexible micro cantilevers in high Knudsen number regimes by theoretical method.

1.2.2 Analysis Issues

This section deals with relevant literature available on the analysis done on AFM models to study the natural, resonant frequency as well as to detect the vibration amplitude variations.

Sedeghi and Zohoor [8] presented the nonlinear vibration analysis for double-tapered AFM cantilever using Timoshenko beam theory and partial differential equations were solved by the differential quadrature method.

Zhang and Murphy [9] presented a multi-modal analysis in the intermittent contact between tip and sample. When AFM is operated in liquids, the methods of actuation and system integration increases the damping.

A first estimate of the distributed lift of thin beam with rectangular cross section is given by Sader [10]. In this work, length to width ratio was selected very large and is subjected to low frequency excitation, so that the beam is locally considered as infinitely long cylinder and fluid loading is analyzed using numerical findings based on unsteady Stokes flow.

Tapping mode (TM) AFM is firstly used by Putman et al. [11]. They successfully measured the frequency responses and tip–sample approach curves of V-shaped silicon nitride cantilevers in both air and liquid.

Korayem et al. [12] showed that the frequency response behavior of microcantilever in liquid is completely different from that in air and studied the influence of mechanical

properties of the liquid like viscosity and density on frequency response analysis. They used finite element method to study the dynamic behavior of AFM in both air and liquid environment. In theoretical modeling, hydrodynamic force exerted by the liquid on the AFM is approximated by hydrodynamic damping. They showed that, microcantilever operating in liquids differs in resonant frequencies from natural frequencies also there is reduction in vibration amplitude. Also they studied the effect of liquid viscosity and liquid density on frequency response. The dynamic behavior of the AFM cantilever under tip sample interaction in both repulsive and attractive regions is analyzed. Then compared the results of finite element simulations with experimental results, which were shown nearly same.

Song and Bhushan [13] used finite element model to know frequency and transient response analysis of cantilevers in tapping mode operating in the air as well as liquid. They approximated hydrodynamic force exerted by the fluid on AFM cantilever by additional mass and hydrodynamic damping. The additional mass and hydrodynamic damping matrices corresponding to beam element is derived. Also numerical simulations are performed for an AFM cantilever to obtain the frequency transient response of the cantilever in air and liquid.

Song and Bhushan [14] has developed a comprehensive finite element model for numerical simulation of free and surface-coupled dynamics of tip cantilever system in dynamic modes of AFM. They did formulation for reflecting the exact mechanism are derived from tapping mode (TM), torsional resonance (TR) and lateral excitation (LE)mode. They suggested that TR and LE modes cannot be ignored as they mostly affects amplitude and phase of cantilever responses.

1.2.3 Experimental Issues

This section deals with relevant literature available on the experiments carried out to know how the environment effects on the atomic force microscopy. And to know the various shapes of cantilever

Lee et al. [15] has discussed the nonlinear dynamic response of atomic force microscopy cantilevers tapping on a sample through theoretical, computational and experimental analysis. They carried out the experiments for the frequency response of a specific microcantilever sample system to demonstrate nonlinearity using modern continuation tools. Also they studied the effect of forced and parametric excitation on bifurcation and instabilities of the forced periodic motions of the microcantilever system.

Hossain et al. [16] demonstrated the dynamic response of microcantilever beams and characterized rheological properties of viscous material. Initially they measured the dynamic response of the mini cantilever beam experimentally which is partially submerged in the air and water for different configurations using a duel channel PolyTec scanning vibrometer. Then they implemented finite element analysis (FEM) method to predict the dynamic response of the same cantilever in air and water, and compared with corresponding experiments. They also conducted numerical analysis to investigate the variation in modal response with changing beam dimensions and fluid properties.

Vancura et al. [17] analyzed characteristics of the resonant cantilever in viscous liquids using rectangular cantilevers geometries in pure water, glycerol and ethanol solution with different concentrations. Their study results can be used in resonant cantilevers as biochemical sensors in liquid environments.

Muramatsu et al. [18] fabricated polymer tips for AFM for study of the effects of tip length and shape on cantilever vibration damping in liquids. They studied the tip sample distance and the normalized vibration amplitude in liquid for the four tips of different length.

Jones and Hart [20] have demonstrated a simple method for utilising the system as a micro viscometer, independently measuring the viscosity of the lubricant for the test. They studied the drag and squeeze film damping effect on microcantilever and discussed cantilever response in water for large range of cantilever speeds. In the more viscous fluids, that the bulk drag and dynamic response of the cantilever become increasingly important.

1.3 SCOPE AND OBJECTIVE

Based on the above literature available, it is found that there is a lot of scope to work with the cantilever design and analysis tasks in an atomic force microscope to get more effective scanning ability. Both the air and liquid media in which these cantilevers are made to operate have affect in the overall resolution and scanning ability.

In this work an attempt is made to model the base excited microcantilever with nano-tip using a lumped and distributed parameter systems. The intermolecular forces are considered during the tapping mode of oscillation. An experiment is carried out on a tiny metallic cantilever sample to know the frequency response characteristics in air. A 3D finite element model is also used to verify the dynamic characteristics. The effect of surrounding liquid media on the tapping mode dynamics of cantilever is tested using available hydrodynamic models.

CHAPTER-2

2. MATHEMATICAL MODELING

This chapter deals with mathematical models used to represent microcantilevers.

2.1 CONTINUOUS SYSTEM MODEL OF MICROCANTILEVER

In continuous system model analysis, beam dynamics and interaction force are two important things. As shown in following Fig. 2.1, probe measurement system moves upward to preset measuring position through the motion of z-scanner.

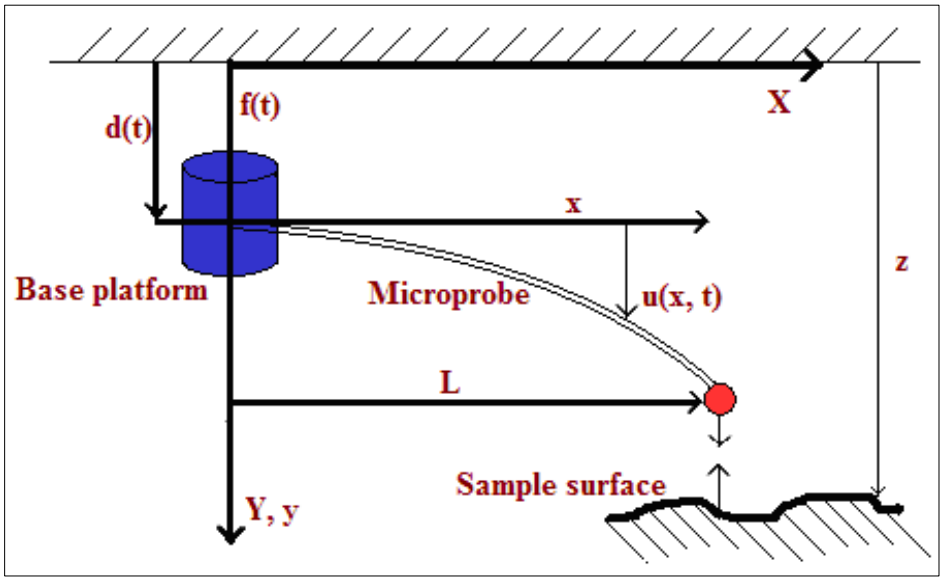

Fig 2.1 Cantilever microprobe

Its end vibrates as a result of straying away from the expected position caused by the deflection of the probe. The probe is a cantilever beam of constant cross-section and fixed to base platform and other end is free. Writing the expressions for kinetic and potential energies respectively as:

$$T = \frac{1}{2}\left\{ m\dot{d}^2(t) + \int_0^L \rho[\dot{d}(t) + \dot{u}(x,t)]^2 dx + m_e[\dot{d}(t) + \dot{u}(L,t)]^2 \right\} \tag{2.1}$$

$$U = \frac{1}{2}\int_0^L EI[u''(x,t)]^2 dx \tag{2.2}$$

where m is mass of z-scanner (base), m_e is mass of probe tip, L is length of probe up to tip, d(t) is displacement of base platform, u(t) is transverse displacement, I is moment of inertia of the probe cross section, ρ is the linear density of the probe. The virtual work done by the non-conservative forces is

$$W=f(t)\, d(t)+F_i\,(t)\{d(t)+u(L,t)\} \tag{2.3}$$

Here f(t) is external force applied at the base, $F_i(t)$ is the interaction force between tip and sample. By using Hamilton's principle, the following equation of motion is obtained:

$$EIu''''(x,t) + \rho\{\ddot{d}(t)+\ddot{u}(x,t)\}=0 \tag{2.4}$$

$$(m+\rho L+m_e)\ddot{d}(t)+\int_0^L \rho\ddot{u}(x,t)dx+m_e\ddot{u}(L,t)=f(t)+F_i(t) \tag{2.5}$$

Here the symbol '''' indicates $\frac{\partial^4}{\partial x^4}$ and double dot superscript represents $\frac{\partial^2}{\partial t^2}$.

The boundary conditions are:

$u(0,t)=0$, $u'(0,t)=0$, $EIu''(L,t)=0$ and

$$EIu''''(L,t) - m_e\{\ddot{d}(t)+\ddot{u}(L,t)\}=F_i(t) \tag{2.6}$$

The nanomechanical interaction force between the probe's tip and sample may be obtained either using Hertz contact model or Derjaguin-Muller-Toporov (DMT) contact model or the Lennard–Jones (LJ) model. For example, Hertz model can be used to express:

$$F_i(t)=-k[d(t)+u(L,t)] \tag{2.7}$$

Where $k=-(6E^*RF_o)^{1/3}$ is a spring constant in which R is radius of the tip (modelled as a sphere), F_o is an interaction force at the equilibrium position and E* is the effective modulus

of tip-sample given by: $E^* = \left[\frac{(1-\nu_t^2)}{E_t} + \frac{(1-\nu_s^2)}{E_s} \right]^{-1}$, where E_t, E_s, ν_t, ν_s are the elastic moduli and Poisson's ratio of the tip and sample respectively. Writing u(x,t)=w(x,t)-d(t), we can express the equations of motion more conveniently as follows:

$$m\ddot{d}(t) + \int_0^L \rho\ddot{w}(x,t)dx + m_e\ddot{w}(L,t) + kw(L,t) = f(t) \tag{2.8}$$

$$m_e\ddot{w}(t) - EIw'''(L,t) + kw(L,t) = 0 \tag{2.9}$$

This model is compared with the well-known point-mass model of AFM microcantilever, which is defined according to the following equations:

$$m\ddot{d}(t) + k_c(d(t) - w(t)) = f(t) \tag{2.10}$$

$$m_{eq}\ddot{w}(t) + k_c(w(t) - d(t)) = F_i(t) \tag{2.11}$$

$$\text{with } k_c = 3EI/L^3 \text{ and } m_{eq} = m_e + \rho L/3 \tag{2.12}$$

In the analysis of continuous system model, following parameters of AFM probe are considered: Material rigidity $EI=3\times10^{-11}$ Nm^2, probe length L=232 μm, mass density $\rho=3.262\times10^{-7}$ kg/m, mass of base platform m=0.001 kg,, mass of probe tip $m_e=3.2\times10^{-12}$ kg, tip radius $R=3\times10^{-7}$ μm and spring constant k=340 N/m. The natural frequencies are obtained from the frequency parameter β_i as: $\omega_i^2=\beta_i^4 EI/\rho$, which is arrived by solving the following equation:

$$\beta_i^3(1+\cos\beta_i L \cosh\beta_i L) + \left(\frac{k}{EI} - \frac{m_e\beta_i^4}{\rho}\right)(\sin\beta_i L\cosh\beta_i L - \sinh\beta_i L\cos\beta_i L) = 0 \tag{5.1}$$

Substituting L and other parameters, we get with MATLAB:

$\beta_1=7.78\times10^3$ and corresponding $\omega_1=579.2\times10^3$ rad/s or 92.1 kHz, where as from eqs. (2.10)-(2.12), by solving eigenvalue problem, we get the natural frequency as: 80.14 kHz. Fig.5.2 shows variation of natural frequency with tip mass ratio.

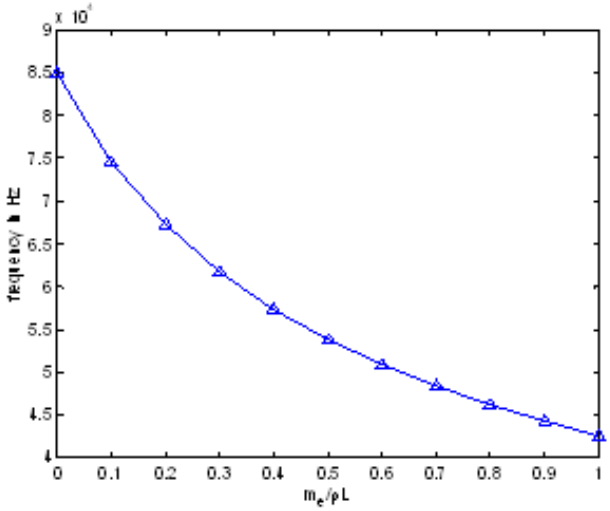

Fig. 2.2 Variation of natural frequency with tip mass

2.2 INTERACTION FORCE MODEL

The interaction between a cantilever tip and sample surface can be modeled as the interaction between a sphere and a flat surface as shown in Fig.2.3.

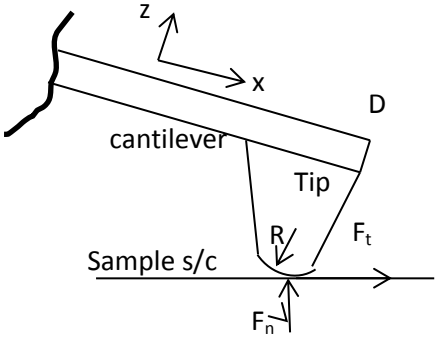

Fig.2.3 Tip-sample interaction

The tip-sample interaction is often modeled by the LJ potential given as

$$U_{LJ}(x,z_0) = \frac{A_1 R}{1260(z_0 + x)^7} - \frac{A_2 R}{6(z_0 + x)} \tag{2.13}$$

where A_1 and A_2 are the Hamaker constants for the attractive and repulsive potentials, respectively. The Hamaker constants are defined as $A_1 = \pi^2\rho_1\rho_2c_1$ and $A_2 = \pi^2\rho_1\rho_2c_2$ in which ρ_1 and ρ_2 are the densities of the two interaction components, and c_1 and c_2 are the interaction constants respectively. Also, z_0 is the equilibrium gap between tip and sample and x(t) is the variable transverse displacement. In this model equivalent radius of the tip is *R*. The LJ force can be defined as the sum of attractive and repulsive forces and expressed as

$$F_{LJ} = -\frac{\partial U_{LJ}}{\partial x} = \frac{A_1 R}{180(z_0 + x)^7} - \frac{A_2 R}{6(z_0 + x)} \tag{2.14}$$

There are other models like DMT, where the interaction between a cantilever tip and sample surface can be modeled as interaction between a sphere and a flat surface just like above. If the long-range attractive force is described by van der Waals force and the short range repulsive force using DMT model, the force calculation is expressed as:

$$F_{DMT}\begin{cases} -\frac{A_1 R}{6x^2}, \text{ for } d_n > a_0 \\ -\frac{A_1 R}{6x^2} + \frac{4}{3}E^*(a_0 - x)^{3/2}\sqrt{R}, \text{otherwise} \end{cases} \tag{2.15}$$

Here *x(t)* is the transient tip-sample separation and a_0 is the intermolecular distance.

2.3 HYDRODYNAMIC FORCES

2.3.1 Beam vibration in liquids

We considered flexural vibration of cantilever beam under harmonic base excitation. Let *x* be the co-ordinates along the beam axis with *y* and *z* are the coordinates along width and thickness. Beam is slender and composed of homogeneous and isotropic material. The classical linear Euler-Bernoulli beam theory gives the equation of motion as:

$$\frac{\partial^2}{\partial x^2}\left[K \times \frac{\partial^2 u(x,t)}{\partial x^2}\right] + (\rho bh) \times \frac{\partial^2 u(x,t)}{\partial t^2} = F_{hyd}(x,t) + S(x,t) + F(t) \tag{2.17}$$

where, $K = \frac{Ebh^3}{12}$ with b and h are width and thickness, ρ=Mass density of cantilever, $u(x,t)$=Beam deflection, $F(t) = F_0 \sin(\omega t)$ = Harmonic base excitation, $S(x,t) = -B\frac{\partial w(x,t)}{\partial t}$ is the damping force, $L =$ Length of beam, $F_{hyd}(x,t)$ describes hydrodynamic action exerted on the beam by the encompassing fluid. The effect of liquid viscosity can be taken care by a simple model. Researchers [eg.,13] have approximated the hydrodynamic forces to be in proportion to the cantilever acceleration and velocity as:

$$F_{hyd}(x,t) = -c_a \frac{\partial u}{\partial t} - \rho_a \frac{\partial^2 u}{\partial t^2} \tag{2.18}$$

Where, c_a = additional hydrodynamic damping coefficient= $\left(3\pi\eta + \frac{3}{4}\pi b\sqrt{2\eta\rho_{liq}\omega}\right)$ and additional mass density $\rho_a = \left(\frac{1}{12}\pi\rho_{liq}b^2 + \frac{3}{4}\pi b\sqrt{\frac{2\rho_{liq}\eta}{\omega}}\right)$. Here, ω is vibrating frequency of the cantilever, η is kinematic viscosity of liquid, ρ_{liq} is density of the liquid.

2.3.2 Solution methodology

Fig.2.4 shows the microcantilever considered with its nomenclature. In order to solve the dynamic equations in continuous form, the Galerkin's approximation method is employed. Here we considered $u(x,t) = \sum_{i=1}^{M} \phi_i(x) q_i(t)$ where M is the number of modes used, $\phi_i(x)$ is its normalized modal function. As the first mode dominates, often $u(x,t)$ is approximated as $\phi_1(x)q_1(t)$. Here, $\phi_1 = \phi_1(x)$ is obtained from the boundary conditions of the beam.

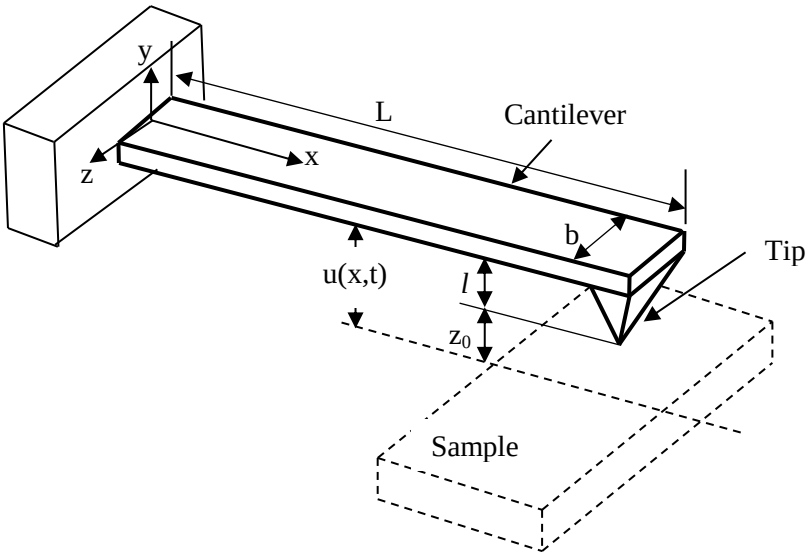

Fig 2.4 Micro-cantilever beam under consideration

The mode shape function $\phi_1(x)$ is multiplied on both sides of the differential eq.(2.17) and the resultant equation is integrated along the cantilever length. i.e.

$$\int_0^L \phi_1 q_1 K \frac{\partial^4 \phi_1}{\partial x^4} dx + (\rho bh + \rho_a)\ddot{q}_1 \int_0^L {\phi_1}^2 dx + (B + c_a)\dot{q}_1 \int_0^L {\phi_1}^2 dx = F_0 q_1 \sin \omega t \int_0^L \phi_1 dx \quad (2.19)$$

In addition to the hydrodynamic and harmonic forces, the system is subjected to an atomic interaction force $f_{ID}(t)$ in microscopic level. The general mode shape function is obtained from the following boundary conditions:

$$\text{At } x = 0\text{: } w(0,t) = 0\text{, and } \frac{\partial w(0,t)}{\partial x} = 0 \quad (2.20)$$

$$\text{At } x = L,\ K\frac{\partial^2 w(L,t)}{\partial x^2} = 0\text{, and } K\frac{\partial^3 w(L,t)}{\partial x^3} = m_e \frac{\partial^2 w(L,t)}{\partial x^2} - f_{ID}(t) \quad (2.21)$$

Here, $f_{ID}(t) = -k_{ts} w(L,t)$ is linearized tip-sample interaction force, with contact stiffness

$$k_{ts} = -\frac{\partial f_{ID}(t)}{\partial w(L,t)} = \begin{cases} -\dfrac{A_1 R}{3 z_0^3}, & if\ (z_0 - w(L,t)) \geq a_0 \\ 2E^* \sqrt{R(a_0 + z_0)}, & if\ (z_0 - w(L,t)) < a_0 \end{cases} \quad (2.22)$$

Here m_e is equivalent tip mass added. The frequency equation and eigenfunction can be obtained from above four boundary conditions as follows (see appendix-IV)

$$2\left[k_{ts} - m_e \frac{EI}{\rho A}\beta^4\right]\left[\sin\beta L \cdot \cosh\beta L - \cos\beta L \cdot \sinh\beta L\right] + 2\beta^3 EI\left[1 + \cos\beta L \cdot \cosh\beta L\right] = 0 \quad (2.23)$$

where $\beta^4 = \frac{\rho A}{EI}\omega^2$. The normalized mode shape is

$$\phi(x) = \frac{1}{N}\left[(\cos\beta L + \cosh\beta L)(\sin\beta x - \sinh\beta x) - (\sin\beta L + \sinh\beta L)(\cos\beta x - \cosh\beta x)\right] \quad (2.24)$$

where

$$N = 2(\sin\beta L\cosh\beta L - \cos\beta L\sinh\beta L) \quad (2.25)$$

Table 1.1 shows the data considered for analysis in MATLAB coding.

Table 1.1 Parameters of simulation for the AFM cantilever [5]

Cantilever length (L)	200 µm
Cantilever width (b)	140 µm
Cantilever thickness (t)	7.7 µm
Cantilever mass density (ρ)	2730 Kg/m^3
Cantilever Young's Modulus (E)	130 GPa
Quality factor of air (Q)	900
Liquid density(ρ_{liq})	1030 Kg/m^3
Liquid viscosity(η)	13.2×10^{-4} Kg/m^3
Tip length(l)	10 µm
Tip radiud(R)	10 nm
Hamarker constant (A_1)	2.96×10^{-19} J
Intermolecular distance (a_0)	0.38 nm
Effective elastic modulus (E^*)	10.2 GPa
Effective elastic modulus (G^*)	4.2 GPa

The computations are performed with a MATLAB 7.10.0 (R2010a) symbolic logic program, which can resolve the equations into ordinary differential form in terms of q_1. Runge Kutta forth order method is used for solving this equation. MATLAB function ode45 is also used which is a variable time-step Runge-Kutta formula necessary to obtain solution of nonlinear equations. MATLAB code employed for this is indicated below:

```
%%%%%%%%%%%%%%%%%%%%%%%%%%%%%%%%%%%%%%%%%%%%%%%%%%%%%%
syms u x
global l b rho th I1 I2 omega u E I Bd
%alp is tip mass ratio
l=200e-6;    %length of microcantilever
b=140e-6;   %width of microcantilever
th=7.7e-6; %thickness of microcantilever
Area=b*th;
I=(b*th^3)/12;
rho=2730;
E=130e9;
alp=0.01; % tip-mass ratio
 % NOTE u=beta*l;
omega=(3.516*sqrt(E*I/(rho*Area))/l^2);% NATURAL FREQUENCY WITH A SIMPLE CANTILEVER
ksy=rho*Area*l*(omega)^2; % microcantilever stiffness
kts=0.1*ksy;%0.0398
me=rho*Area*l*alp;
Bd=2*sqrt(ksy/me)*0.05;% Corresponding to Q=1000
p1=me*E*I/(rho*Area*l^4);%=3.2196e-004
p2=2*E*I/l^3;%=0.0644
u=1.8;
%TO SOLVE THE TRANCEND. EQ. IN TERMS OF u WE USE NEWTON-Raphson'S METHOD FOR WHICH
DIFFERENTIAL IS REQUIRED
 for i=1:50
   freq=2*(kts-p1*u^4)*(sin(u)*cosh(u)-cos(u)*sinh(u))+p2*u^3*(1+cos(u)*cosh(u));
   dfreq=-8*p1*u^3*(sin(u)*cosh(u)-cos(u)*sinh(u))+2*(2*kts-
2*p1*u^4)*sin(u)*sinh(u)+3*p2*u^2*(1+cos(u)*cosh(u))+p2*u^3*(-sin(u)*cosh(u)+cos(u)*sinh(u));
   u=u-freq/dfreq;
end
display(u^2);
omega1=(u/l)^2*sqrt((E*I)/(rho*Area)); % NATURAL FREQUENCY WITH EQUIVALENT INTERACTION SPRING
AND TIP-MASS BOUNDARIES

% DEFINITION OF MODE SHAPE FUNCTION
N=2*(sin(u)*cosh(u)-cos(u)*sinh(u));
A=(cos(u)+cosh(u))/N;
B=-(sin(u)+sinh(u))/N;
C=-(cos(u)+cosh(u))/N;
D=(sin(u)+sinh(u))/N;

phi=A*sin(u*x/l)+B*cos(u*x/l)+C*sinh(u*x/l)+D*cosh(u*x/l);
I1=eval(int((phi*phi),0,l));
I2=eval(int(phi,0,l));

%SOLVING THE DIFFERENTIAL EQUATION
dt=1e-5;
tspan=0:dt:5;
q0=[0.0001;1e-3];
[t,q]=ode45(@cs, tspan, q0);
plot(q(:,1),q(:,2));
xlabel('displacement of cantilever'); ylabel('velocity of the cantilever');

%%%%%%%%%%%%%%%%%%%%%%%%%%%%%%%%%%%%%%%%%%%%%%%%%%%%%%
```

Various forces considered for obtaining the response from above coding are given in the following MATLAB function:

```
============================================================
function f1 = cs(t, x)
global l b rho th I1 I2 u E I Bd omega

f0=1; % UNIT AMPLITUDE TIP HARMONIC EXCITATION
Ks=E*I;
omega2=1e6; % EXCITATION FREQUENCY IN RAD/S
nita=13.2e-4; %VISCOSITY OF THE LIQUID
rhliq=1030; %DENSITY OF  LIQUID ENVIRONMENT
Ca=3*pi*nita+(3/4)*pi*b*sqrt(2*nita*rhliq*omega); %ADDITIONAL HYDRODYNAMIC DAMPING COEFFICENT
rhoa=((1/12)*pi*rhliq*b^2)+(3/4)*pi*b*sqrt(2*rhliq*nita/omega); %ADDTITIONAL MASS DENSITY
%mm=1/(rho*b*th+rhoa); %1.1499e+5
mm=1.1499e3;
%STATE SPACE REPRESENTATION OF THE SYSTEM.
f1=zeros(2,1);
f1(1)=x(2);
f1(2)=(-((u^4)*mm*Ks*I1*x(1))-(Bd+Ca)*mm*I1*x(2)+f0*mm*I2*sin(omega2*t)*x(1));
return
=====================================================
```

First the frequency equation is solved and results are shown. The effect of equivalent linear interaction stiffness: $\hat{k}_{ts} = k_{ts}/k$, where $k=\rho A l \omega_n^2$ on natural frequencies is as shown in Fig. 2.5 both with and without tip-mass.

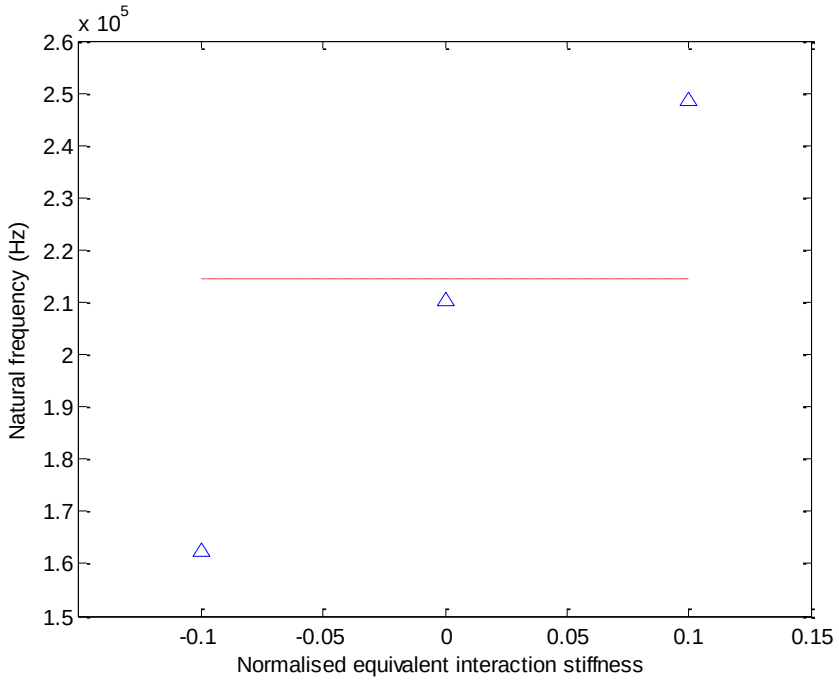

Fig 2.5 Natural frequency versus normalized interaction stiffness

Here, the dotted line indicates the natural frequency of normal cantilever in air without tip mass. It is seen that even if interaction stiffness is zero, the natural frequency mismatch with dashed line is due to the tip-mass boundary condition. Quality factor is defined as $Q = \frac{\omega \rho A l}{B}$, where B is damping coefficient. For constant values of mass and damping coefficient it is a function of natural frequency. Fig.2.6 shows the variation of quality factors with interaction stiffness (negative for attraction, zero for free oscillation and positive for repulsive interaction).

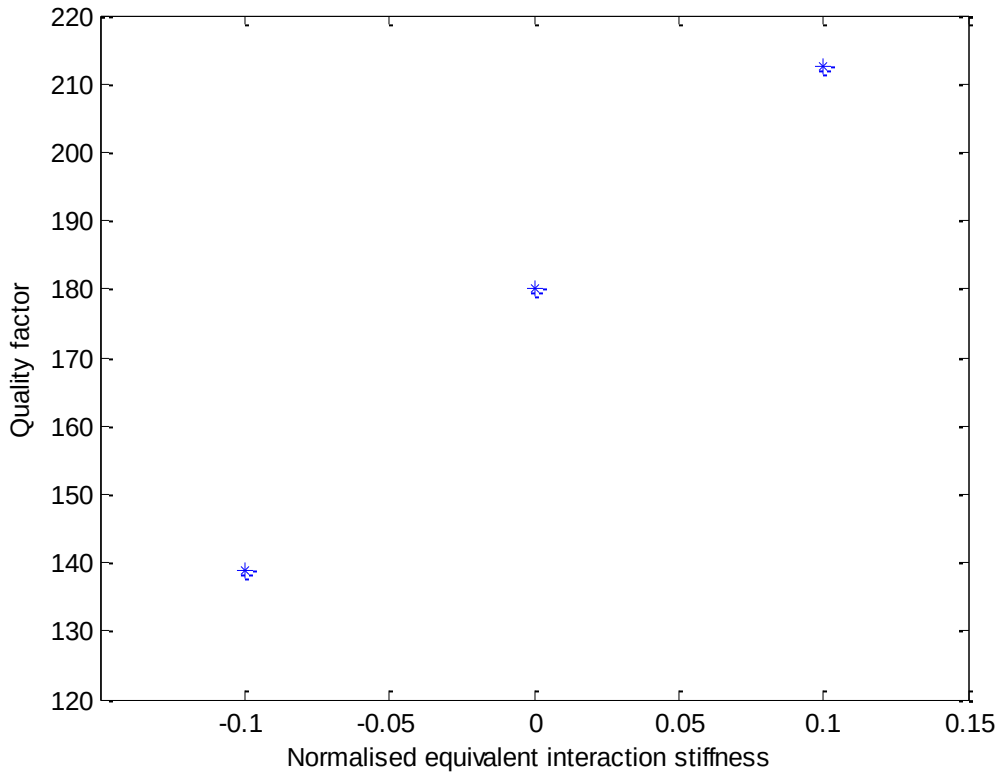

Fig.2.6 Quality factor Q vs Normalized interaction stiffness

The viscous damping ratio considered in present work is 0.05.

The differential equations are solved and Fig.2.7 shows the time history with $\hat{k}_{ts}$ =0.1.

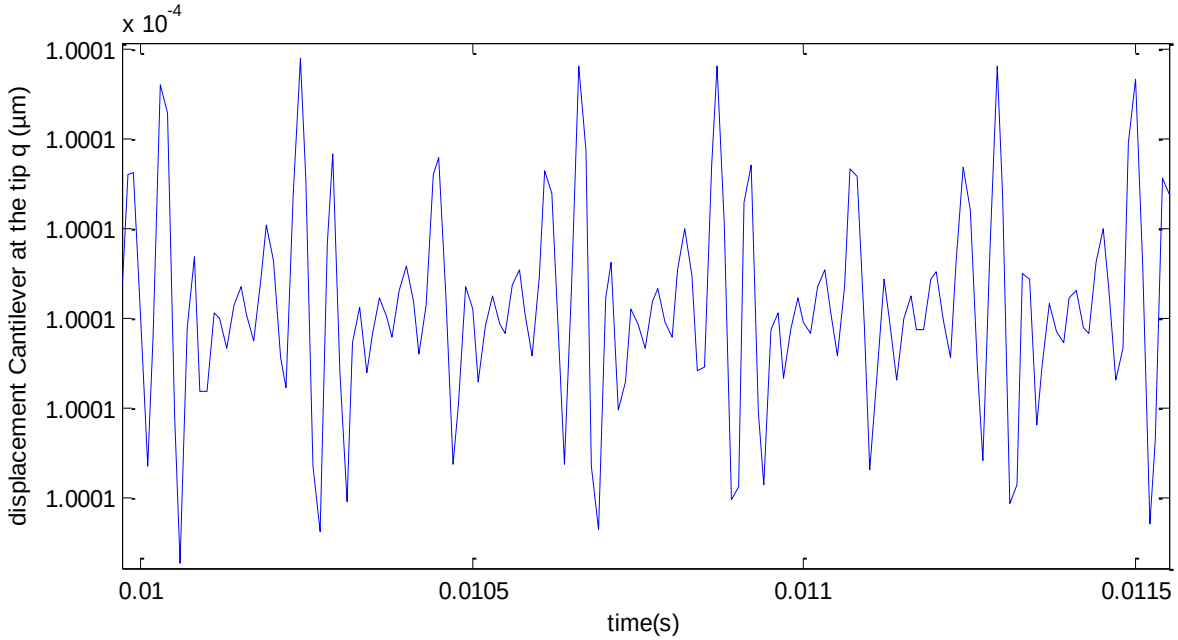

Fig 2.7 Variation of the displacement(µm) of system with respect to time (s)

Fig.2.8 shows the corresponding phase diagram, which indicates a chaotic state.

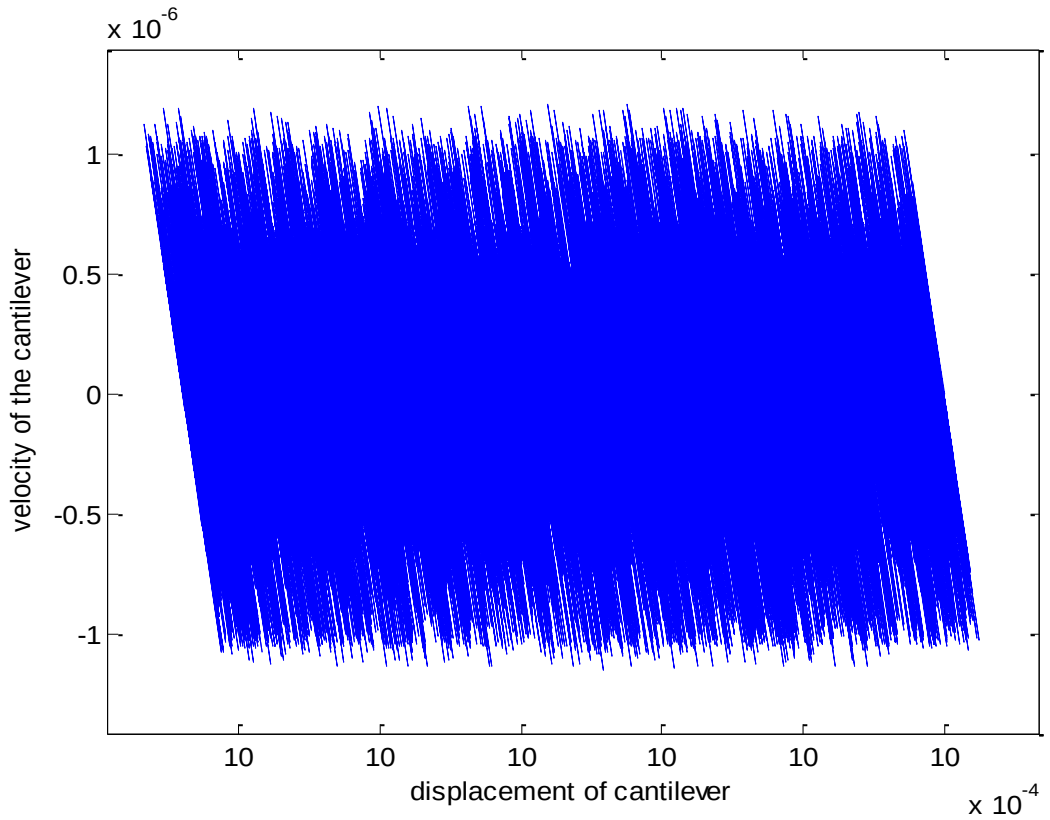

Fig. 2.8 Graph of displacement vs. velocity of the cantilever.

2.4 LUMPED PARAMETER MODELING

This model of a spring mass system is considering circular tip at the end of cantilever. System is being run in tapping mode and effects of the LJ potential force, squeeze film damping force are predicted. During the AFM operation in the TM, a low-dimensional model reduction can provide an accurate description of the cantilever dynamics. The cantilever is driven by the harmonic driving force, the tip-sample interaction force F_{LJ} (LJ force) and the force due to squeeze film damping F_s. The governing equation of motion of the cantilever subjected to base harmonic force $f_0 \cos(\omega t)$ can be written as

$$m\ddot{x} + c\dot{x} + kx + k_3x^3 = F_{LJ}(x, z_0) + F_s(x, \dot{x}, z_0) + f_0 \cos \omega t \tag{2.26}$$

where x is the instantaneous displacement of the cantilever tip measured from the equilibrium tip position in the absence of external forces with positive values toward the sample surface, ẋ and ẍ are the instantaneous velocity and acceleration of the cantilever tip, m, k and c are the equivalent mass, spring stiffness and damping coefficients of the cantilever in the air. The constant k_3 is nonlinearity in the system as cubic stiffness. Solving this second order partial differential equation with Runge-Kutta method, we can study the effect of nonlinearity, damping forces and frequency of oscillation. The results for this analysis are shown with the numerical data depicted in Table-1.2[3]:

Table 1.2 Input data for lumped parameter model [3]

Property	**Value**
Length	449µm
Width	46µm
Thickness	1.7µm
Tip radius	150nm
Material density	2,230kg/m3
Young's Modulus	176GPa
Bending stiffness	0.11N.m-1
Quality Factor	100
Hamaker constant(Rpulsive)	1.3596×10-70J.m6
Haaker constant (attractive)	1.856×10-19J

The coding developed in MATLAB is as follows

```
%%%%%%%%%%%%%%%%%%%%%%%%%%%%%%%%%%%%%%%%%%%%%%%%%%%%%%%%
dt = 1e-6;
tspan = [0:dt:0.01];
y0 =[0 0];
[t y]=ode45(@func,tspan,y0);
plot(y(:,1), y(:,2));
xlabel('x');
ylabel('$\dot x$','interpreter','latex');
y1=y(:,1);
Fs=1/dt;
L=length(y1);
NFFT=2^nextpow2(L);
y1f=fft(y1,NFFT)/L;
fre=Fs/2*linspace(0,1,NFFT/2+1);
figure
plot(fre,(2*abs(y1f(1:NFFT/2+1))));
xlabel('Frequency');
ylabel('Amplitude');
%%%%%%%%%%%%%%%%%%%%%%%%%%%%%%%%%%%%%%%%%%%%%%%%%%%%%%%%%%
```

Various forces considered in lumped parameter model for obtaining the response from above coding are given in the following MATLAB function:

```
function
L=449e-6;
B=46e-6;
H = 1.7e-6; % height of cantilever
Ro = 2330;
mass = Ro*L*B*H;
F0 = 1;
k = 0.11;
omegan= sqrt(k/mass);
omega=omegan*0.5;
Q = 100;
eta = 1/(2*Q);
Cc = 2*sqrt(k*mass);
C = eta*Cc;
beta = 0.42;%
A1 = 1.3596e-70;
A2 = 1.865e-19;
R = 150e-6;
D = (A2*R)/(6*k);
Zs = 1.5*(2*D)^1/3;
kc = 2; %(beta*k)/(Zs^2);
alfa = 1.2;
z0 = 1;%alfa*Zs;
mu = 18.3e-6;
Pa = 1.013e-5;
L0 = 65e-9;
P0 = 0.8*133.32;
Kn = Pa*L0/(P0*(z0-x(1)));
mueff = mu/(1+9.638*Kn^1.159);
m = 1/mass;
f = zeros(2,1);
f(1) = x(2);
f(2) = m*(F0*cos(omega*t)-C*x(2)-kc*x(1)^3-k*x(1)+A1*R/(180*(z0+x(1))^8)-
A2*R/(6*(z0+x(1))^2)+x(2)*mueff*B^3*L/(x(1)+z0)^3);
return
================================================================
```

Results obtained from the program for lumped parameter model are as follows: Fig.2.9 shows a phase diagram for the harmonically excited linear system with interaction force.

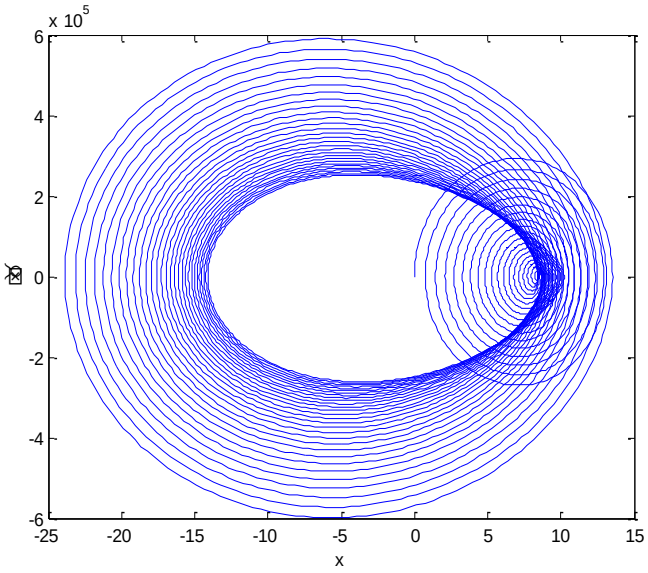

Fig.2.9 Linear system with harmonic excitation

From this phase diagram we observed that the system is stable when only harmonic force exists in the system.

The corresponding FFT is shown in Fig.2.10.

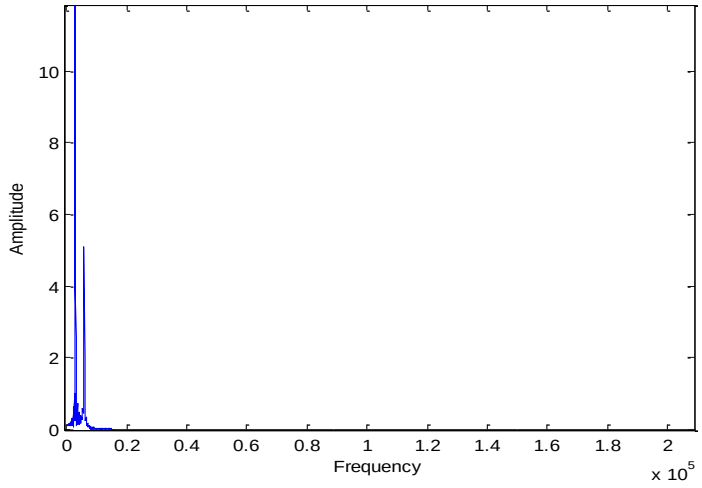

Fig 2.10 Frequency response with harmonic base motion

Fig.2.11 shows a phase diagram for both harmonic force and the interaction LJ potential force.

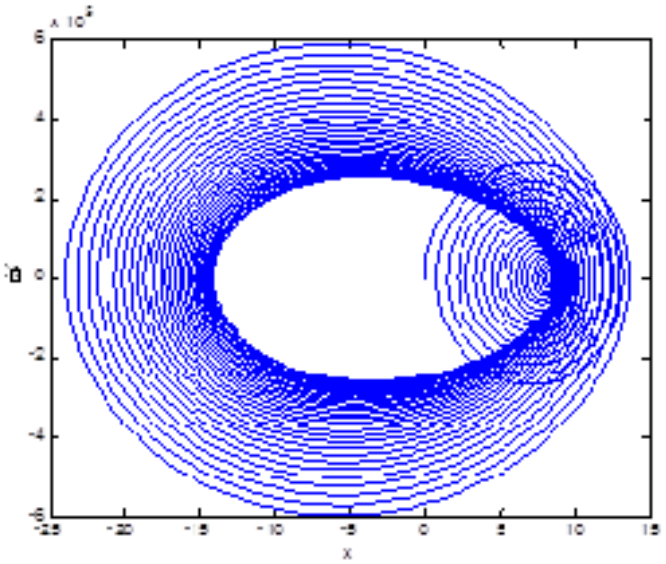

Fig 2.11 System under both harmonic loads and interaction forces

In addition to harmonic force, when interaction forces incorates in the system the system is still behaves as a stable system.

The corresponding frequency response is illustrated in Fig.2.12

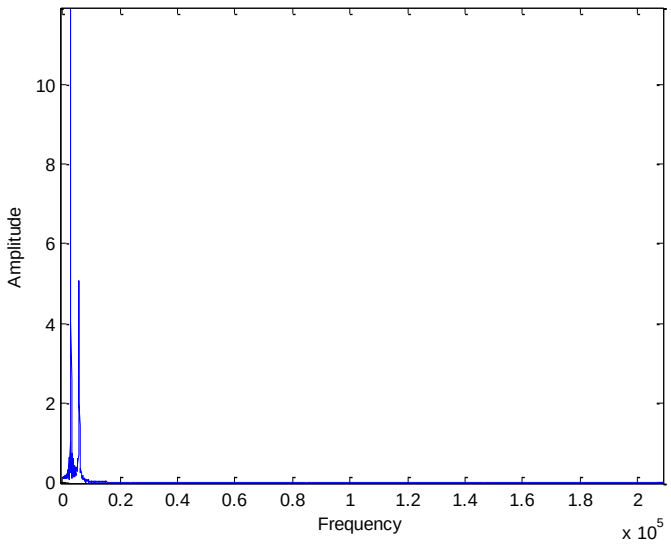

Fig 2.12 Frequency response under harmonic loads and interaction forces

Fig. 2.13 shows the phase diagram of the model with harmonic force with LJ potential and squeeze film damping force

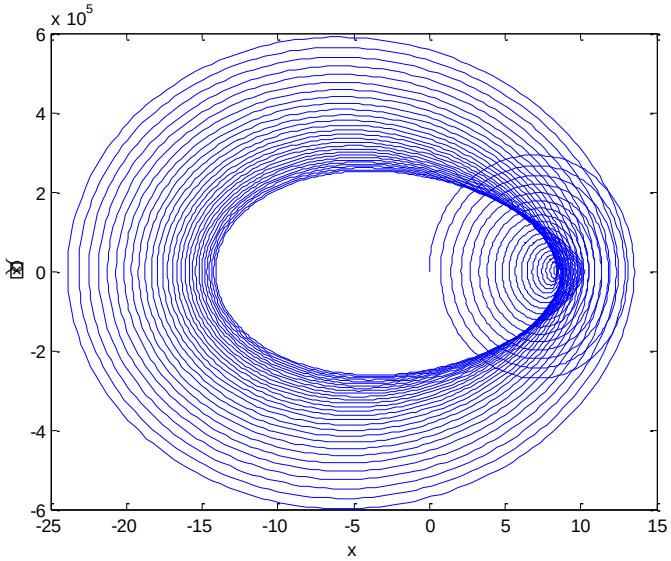

Fig 2.13 System under harmonic force, LJ potential force, squeeze film damping

When we consider the LJ potential force in the system with harmonic force and interaction force, we can see from phase diagram system is stable.

Corrousponding FFT is shown in the fig.2.14.

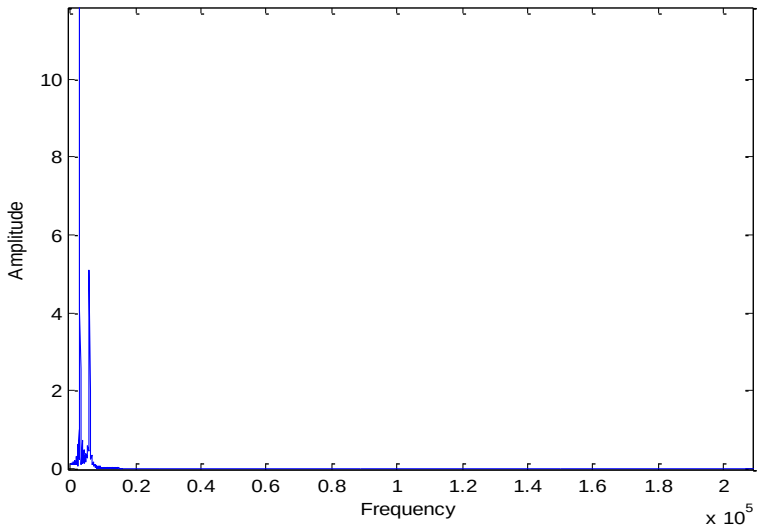

Fig 2.14 Frequency response when system is under harmonic force,
LJ potential force and squeeze film damping

When the system has nonlinearity also (k_3=2 N/m^3) and is subjected to harmonic force with LJ potential and squeeze film damping, the phase diagram is a chaotic attractor as shown in Fig.2.15.

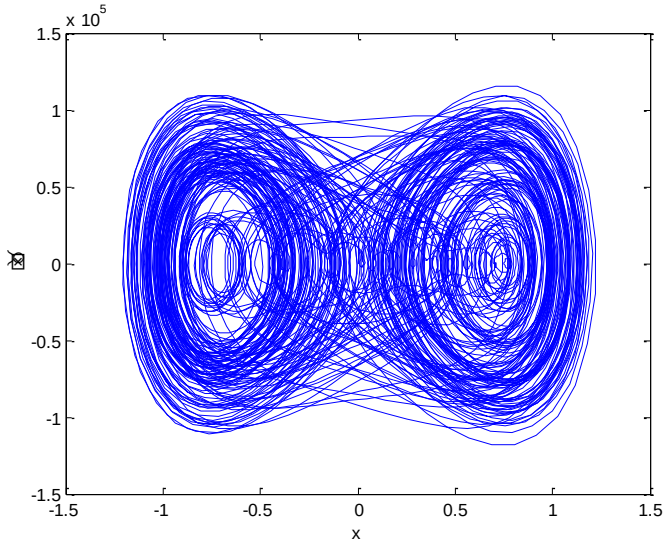

Fig 2.15 System under all forces

Corresponding frequency response change in FFT is shown in the Fig. 2.16

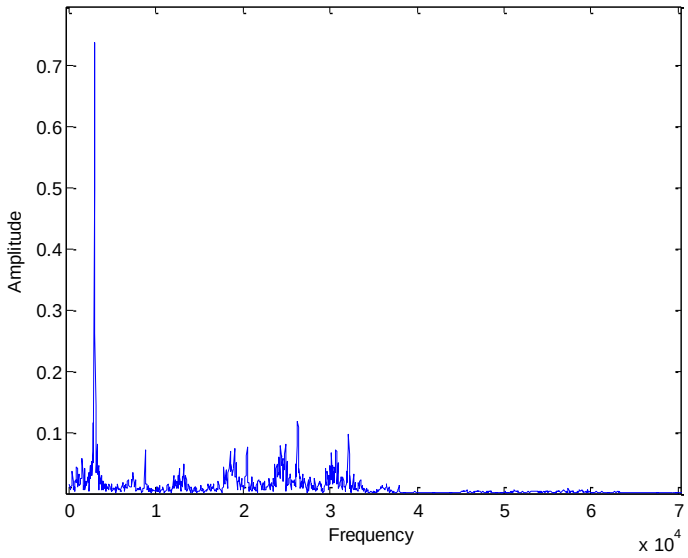

Fig 2.16 Fast Fourier Transform

CHAPTER 3

3. FINITE ELEMENT MODELING

This chapter presents the analysis of base excited microcantilever using finite element modeling. Both one dimensional and three dimensional finite element models are used to represent the AFM cantilever structure.

3.1 BEAM ELEMENTS

Dynamic analysis of AFM cantilevers under tip sample interaction can be done using a finite element model. In this one-dimensional FE model for AFM cantilever system, the microcantilever is discretized by beam element and tip is modeled as rigid mass element. It is assumed that tip was located exactly at the end of the cantilever. Fig.3.1 shows the beam element under consideration.

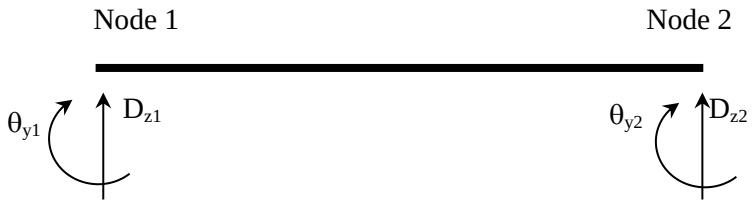

Fig.3.1 Beam element

At the simplest level, cantilever is descritized into two elements. There are two degrees of freedom (DOFs), one displacement and another one rotation as seen from Fig.3.1. The element nodal displacement vector is

$$d^e = \{d_{z1}, \theta_{y1}, d_{z2}, \theta_{y2}\}^T \tag{3.1}$$

Corresponding element nodal force vector consists of shear force and one moment at each node is

$$f^e = \{F_{z1}, M_{y1}, F_{z2}, M_{y2}\} \tag{3.2}$$

For beam element with a length of L_e, the element mass damping and stiffness matrices are expressed as

$$m^e = \int_0^{L_e} \rho A N^T N dx \tag{3.3}$$

$$c^e = \int_0^{L_e} c N^T N dx \tag{3.4}$$

$$k^e = \int_0^{L_e} E I_y \frac{d^2 N^T}{dx^2} \frac{d^2 N}{dx^2} dx \tag{3.5}$$

where N is a cubic Hermite shape function vectors. The FE motion equation of cantilever operating in TM mode in air reduces to:

$$M\ddot{u} + C\dot{u} + Ku = F_{ts} - MI_z \ddot{g}_z(t) \tag{3.6}$$

Here u, $\dot{u}$, $\ddot{u}$ are the system relative displacement, velocity and acceleration vectors, respectively. F_{ts} is the force vector due to the tip sample interaction. And M, C and K are the global mass, damping and stiffness matrices for cantilever vibrating in the air and are obtained by assembling the contributions from the all the beam elements. Matrices M and K are given by

$$m^e = \rho A \begin{bmatrix} 13L_e/35 & -11L_e^2/210 & 9L_e/70 & 13L_e^2/420 \\ -11L_e^2/210 & L_e^3/105 & -13L_e^2/420 & -L_e^3/140 \\ 9L_e/70 & -13L_e^2/420 & 13L_e/35 & 11L_e^2/210 \\ 13L_e^2/420 & -L_e^3/140 & 11L_e^2/210 & L_e^3/105 \end{bmatrix}$$

$$k^e = EI_y \begin{bmatrix} 12/L_e^3 & -6/L_e^2 & -12/L_e^3 & -6/L_e^2 \\ -6/L_e^2 & 4/L_e & 6/L_e^2 & 2/L_e \\ -12/L_e^3 & 6/L_e^2 & 12/L_e^3 & 6/L_e^2 \\ -6/L_e^2 & 2/L_e & 6/L_e^2 & 4/L_e \end{bmatrix}$$

The viscous damping matrix c^e is a linearly proportional matrix of m^e and k^e. The FE model motion equation of cantilever operated in TM and immersed in liquid are modified as:

$$M\ddot{u} + C\dot{u} + Ku = F_{ts} - MI_z\ddot{g}_z(t) + F_d \tag{3.7}$$

Here $F_d = -M_a\left(\ddot{u} + \ddot{b}\right) - C_a\left(\dot{u} + \dot{b}\right)$=the hydrodynamic force vector. By putting F_d in above eq. (3.7) we get simplified form as:

$$\left(M + M_a\right)\ddot{u} + \left(C + C_a\right)\dot{u} + Ku = F_{ts} - \left(M + M_a\right)\ddot{b} - C_a\dot{b} \tag{3.8}$$

Assuming F_{ts} = 0, b = $b_0\sin(\omega t)$, u = $u_0\sin(\omega t) = u_0 e^{i\omega t}$

$$\left[K - \left(M + M_a\right)\omega^2 + j\omega\left(C + C_a\right)\right]u_0 = \left(M + M_a\right)\omega^2 b_0 - jC_a\omega b_0 \tag{3.9}$$

$$\frac{u_0}{b_0} = FRF = K^{*-1}\left[\left(M + M_a\right)\omega^2 b_0 - jC_a\omega b_0\right] \tag{3.10}$$

Where

$$K^* = \left[K - \left(M + M_a\right)\omega^2 + j\omega\left(C + C_a\right)\right] \tag{3.11a}$$

$$M_a = \frac{\rho_a}{\rho}M \tag{3.11b}$$

$$C_a = \frac{C_\infty}{\rho A}M + \frac{\eta b^3}{h^3\rho A}M \tag{3.11c}$$

In the above eq. *h* refers to transient distance between and surface which depends on angle and length of the tip (*l*). In present case *h = l+u.* The results of frequency response analysis are obtained from a simple MATLAB code which assembles element matrices and computes the amplitudes at various values of ω. Fig.3.2 shows the FRF plot for the cantilever in air & liquid (water) along with the other properties considered as in Table 3.1.

Table 3.1 Properties of cantilever and liquid considered [13]

Property	Value	Property	Value
Beam length	252 µm	Density of liquid	1000 kg/m^3
Beam width	35 µm	Elastic modulus	1.3×10^{11} N/m^2
Thickness	2.3 µm	Kinematic viscosity	8.54×10^{-4} kg/ms
Tip mass ratio	0.05	Intermolecular distance (a_0)	0.38 nm

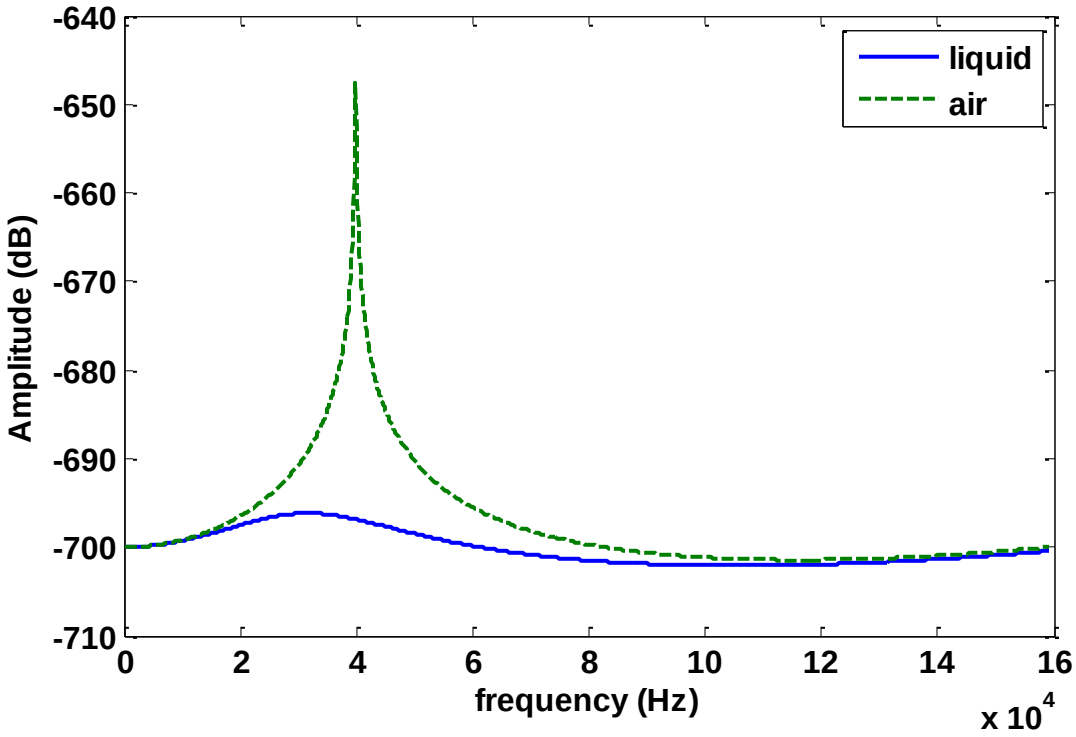

Fig.3.2 FRF plot of the microcantilever with 2 elements operating in liquid and air

It is seen that resonance in air occurs at around 40KHz and it drops inside the liquid environments due to hydrodynamic damping. The additional inertia has little effect.

3.2 SOLID ELEMENTS

The cantilever with known dimensions is modeled in commercial software CATIA V5 R19. Fig 3.3 shows the image of cantilever part modeled with the dimensions mentioned in Table 3.1. The commands used during modeling are Rectangle, Pad, and draft. This CATIA part is used further analysis.

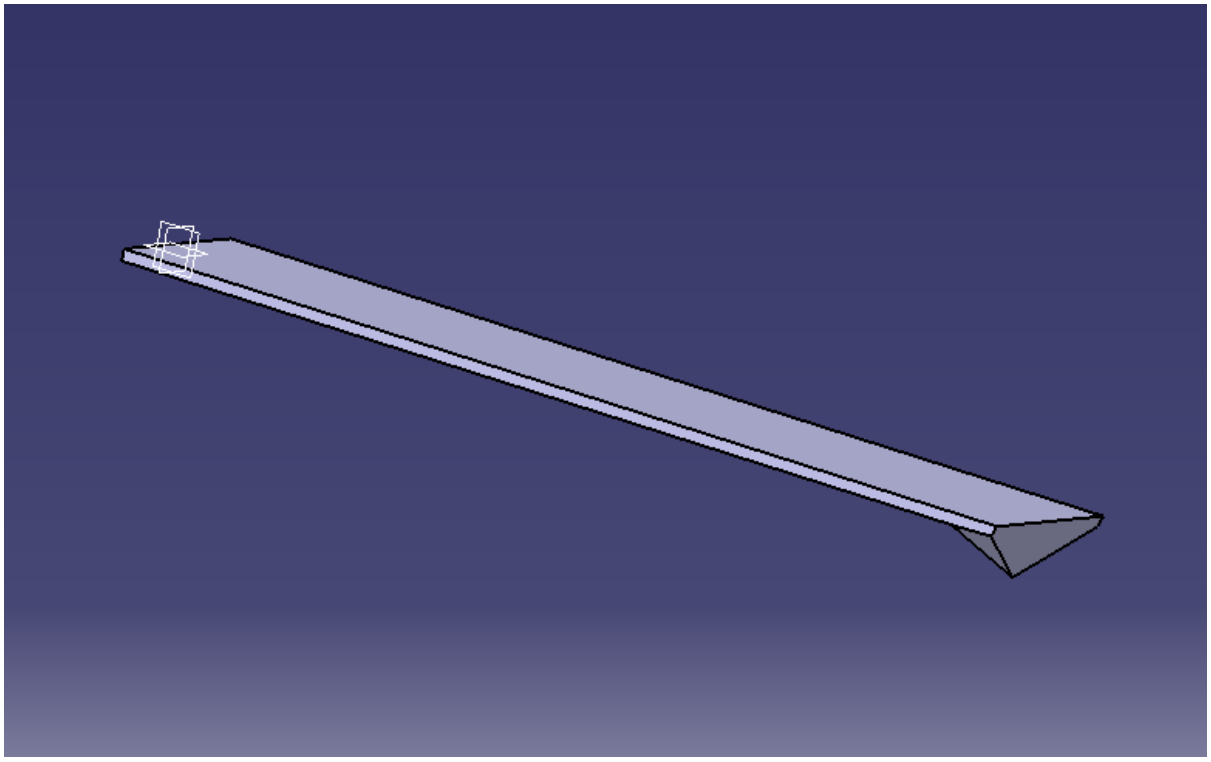

Fig 3.3 Solid model of a microcantilever with nano tip.

3.3 DETAILS OF MESHING

The commercial software ANSYS 14.0 is available for finite element analysis, is used to develop the finite element model of the beam which is under consideration. The CATIA part is imported using command import in ANSYS for further study. As the CATIA part is imported, the material properties are given from the ANSYS library. It is meshed in ANSYS using SOLID185 (8 noded brick with three degrees of freedom at each) elements. The beam is fixed at one end. Its modal analysis gives natural frequencies and corresponding mode shapes when operating in air. The fluid region between the cantilever and substrate surface is modeled by FLUID80 elements. This element is suitable for fluid solid interaction problems. The solid and fluid elements at the interface share same node. Fluid 80 element has three degrees of freedoms per node (u_x, u_y, u_z) and in total there are 8 nodes. The following boundary conditions are applied for the fluid region. 1) $u_x = 0$ for the fluid nodes located at the left most and right modes located. 2) $u_y = 0$ for the fluid nodes located at bottom most

plane. 3) $u_z = 0$ for the fluid nodes located at the leftmost and right most planes (front to back) as seen in Fig.3.4.

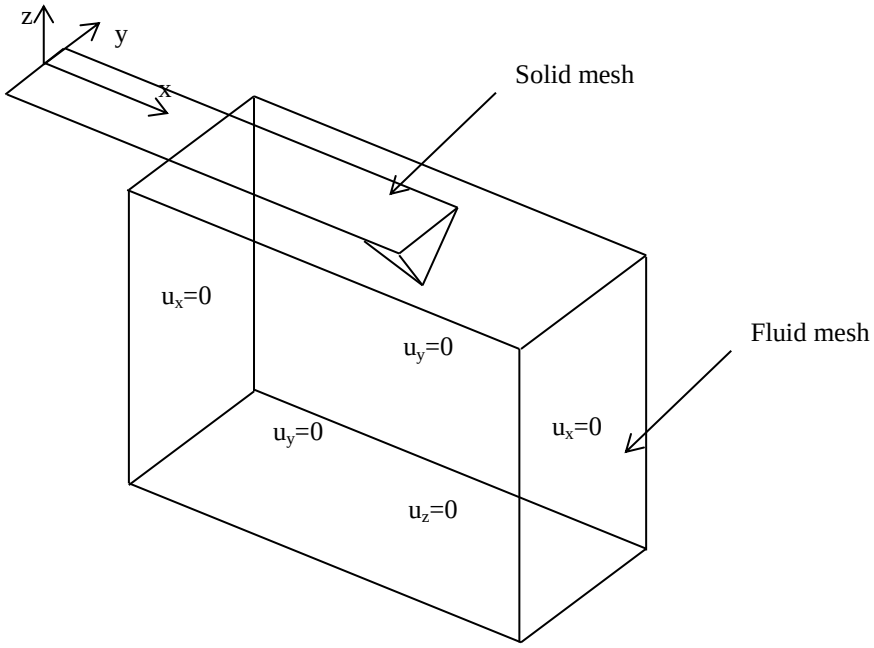

Fig.3.4 Boundary conditions of fluid mesh

The finite element model is shown in the fig 3.5 with the beam fixed at one end.

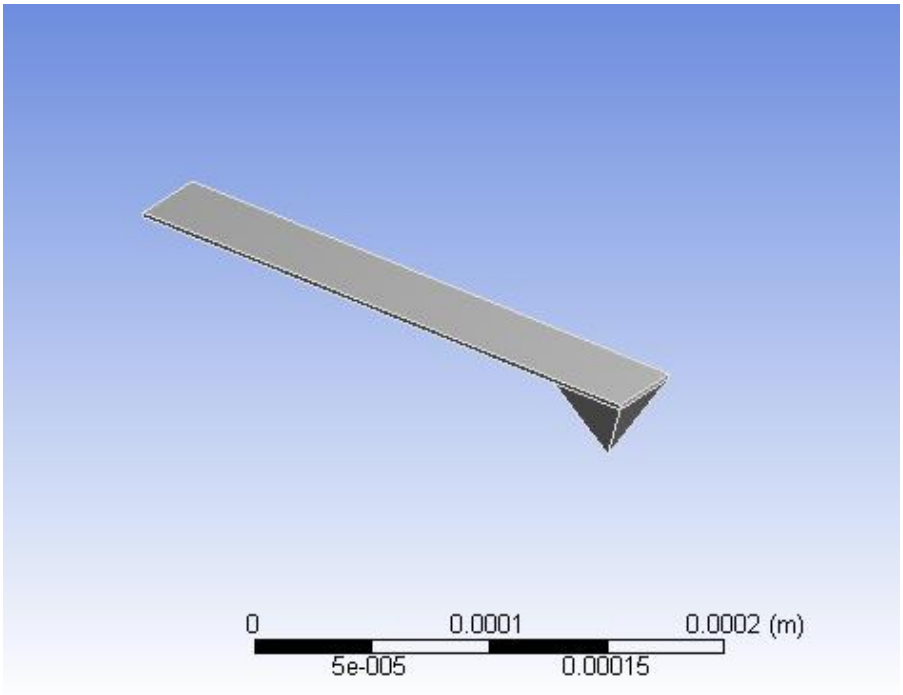

Fig 3.5 Geometry of the cantilever ANSYS 14.0 workbench

After the geometry is made, meshing is done for the analysis of microcantilever in first air and then in water. Boundary conditions are given accordingly, one end is fixed and other end containing tip free to move. Then it is solved for modal analysis and the approximate natural frequency is correlated as 41,000 Hz. Fig.3.6 shows the meshing screenshot of ANSYS for liquid medium.

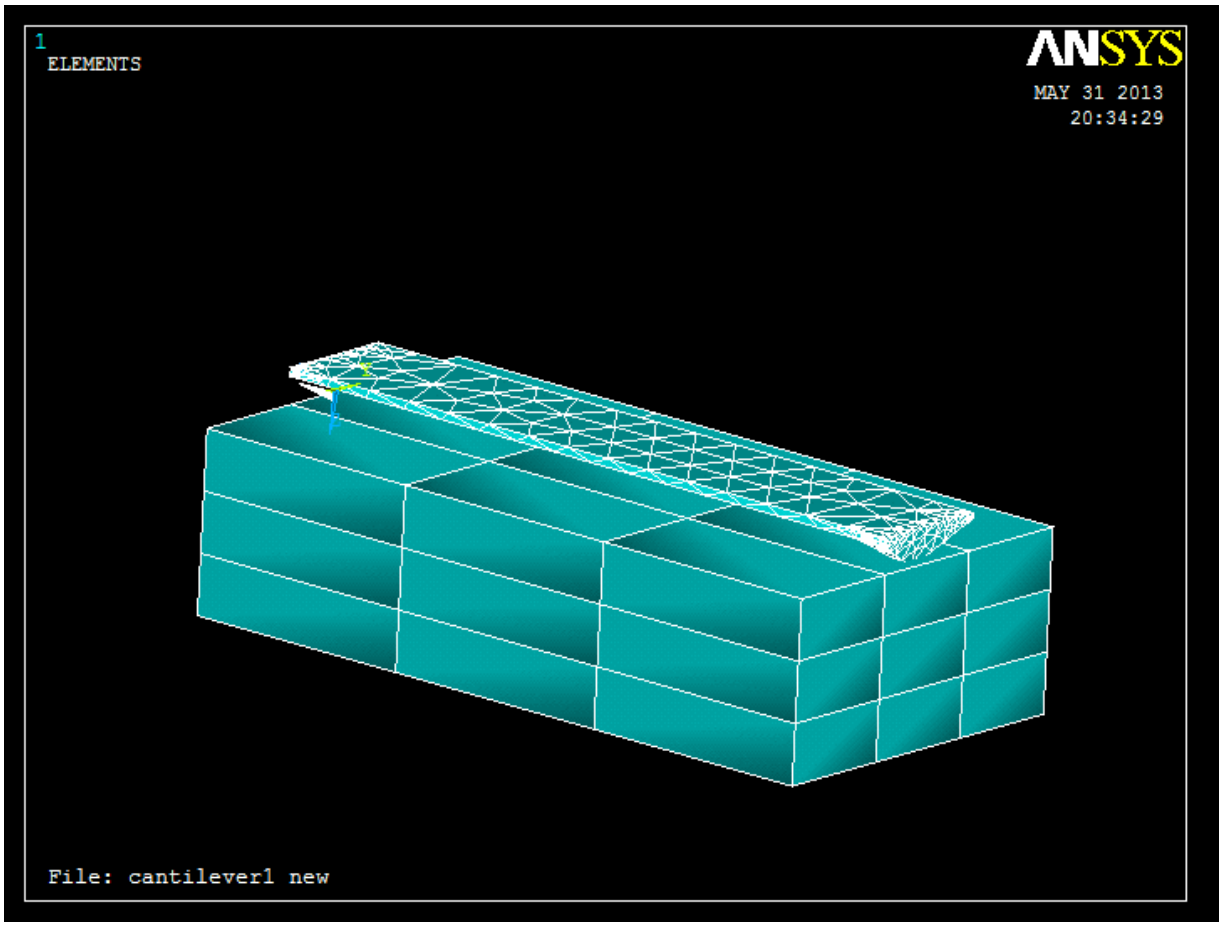

Fig 3.6 Screen shot of meshing for liquid medium

The density and kinematic viscosity of water are entered for the lower region additionally considered. The hexahedral mesh is employed. The fluid boundary conditions are also incorporated. On modal analysis, it is found several other lower modes (due to fluid effect) before reaching the natural frequency of structure at 31,299 Hz.

Fig.3.7 shows the corresponding mode shape of the beam.

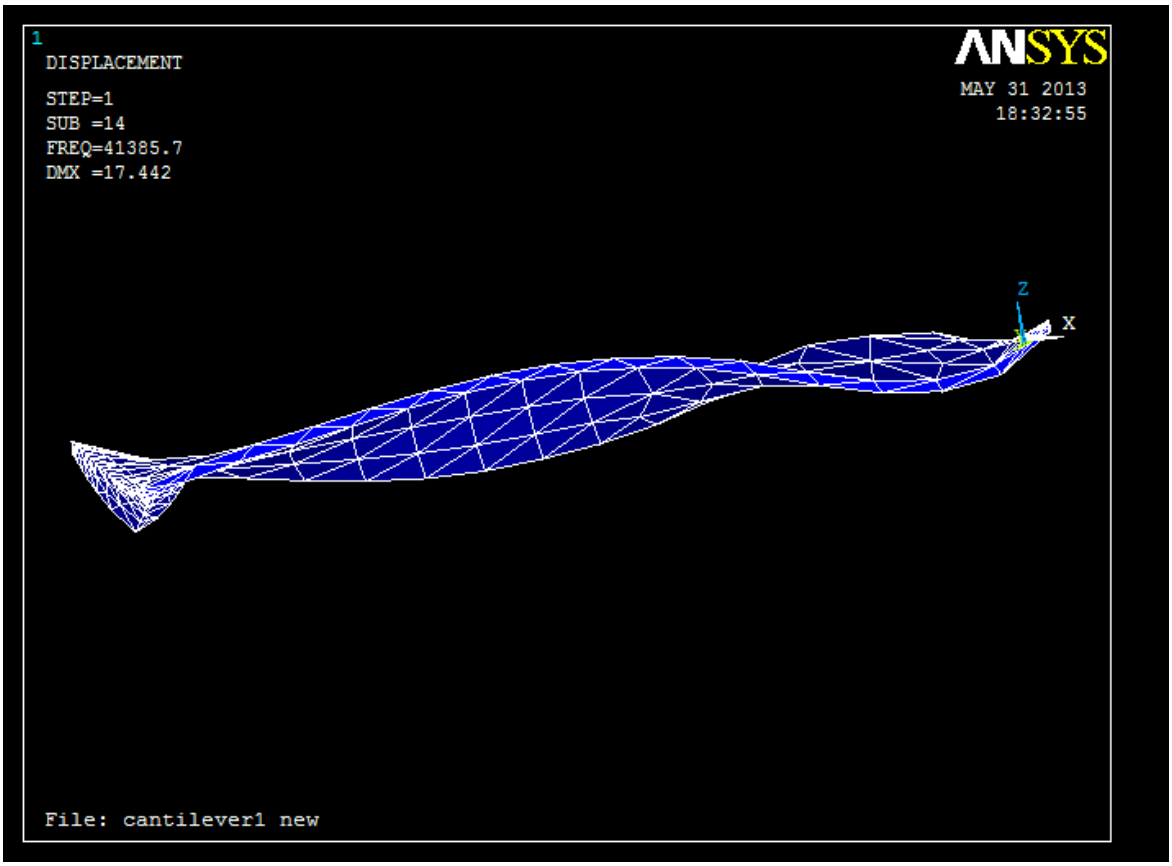

Fig 3.7 Mode shape of the beam.

This analysis has not taken care of any intermolecular forces into account. The effect of hydrodynamic forces is therefore clearly illustrated.

CHAPTER 4

4 EXPERIMENTAL ANALYSIS

This chapter presents the experimental details carried out in this work. Even experiments are not carried out at micro scale, a mesoscale alloy-steel specimen is considered to know the behaviour with base excitation. The sample is obtained from a wire-cut EDM machine and its micro structural analysis is firstpredicted from a scanning electron microscope (SEM).

4.1 DYNAMIC TESTING AND SAMPLE PREPARATION

Apart from the sample obtained from wire-cut EDM machine, another sample is also prespared on a rough scale. Fabrication process started with fabrication of mini-cantilever beam. We took a thin plate for making the mini cantilever beam of 35mm in length, 5mm in width, 1mm in thickness. By using grinding wheel we reduced the width of an aluminium plate for getting defined shape. Then by using hammer it is flattened to required thickness. And then filed using small files for getting smooth surface area. Sample specimen micro-cantilever and mini-cantilever is as shown in the fig. 4.1.a and b.

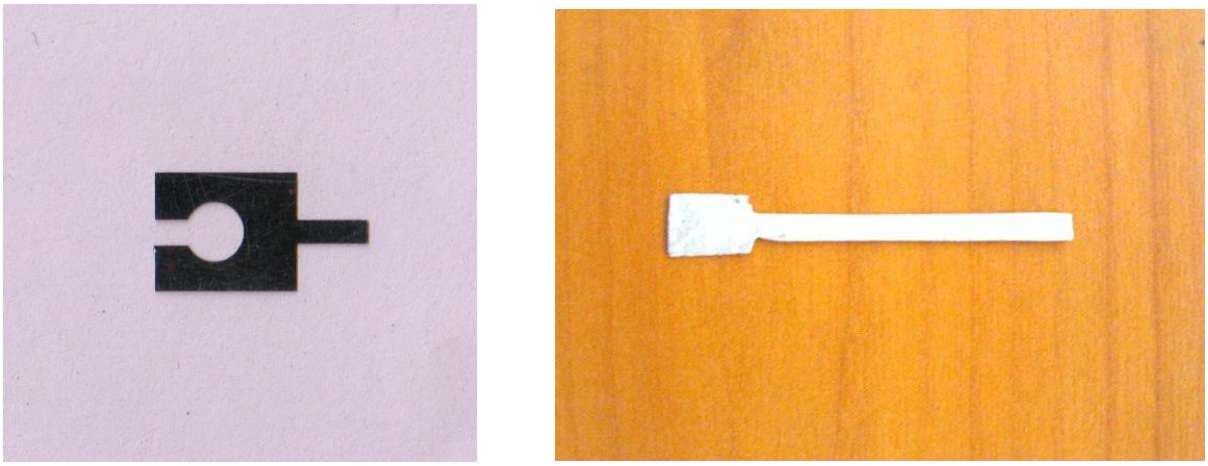

Fig. 4.1. a) Microcantilever beam b) Minicantilever beam

After then the small spherical ball is fixed on the tip of the cantilever. Thus, the cantilever beam with a tip mass is fabricated for doing the experiment.

Before doing experimental setup we started with mounting base preparation. We prepared the base in a workshop, to get the exact dimensions of the base it is filed as well as drilled at center for fixing purpose and then the base is fixed on the stringer of the exciter.

4.2 SEM ANALYSIS

The microcantilever used is tested under scanning electron microscope JSM 6480 LV in metallurgy laboratory. This SEM has two attachments one is coating machine and another one is EDX part. Coating machine is used to coat the sample therefore it will become conducing, so that it can be used to scatter the electrons. EDX part is used to study the chemical composition of the sample. From this SEM we get two types of images: Back electron scattered (BES) and Secondary electron image (SEI). From BES we can see different phases and elements in sample. From SEI we can identify different composites available in the sample.different parameters set for study our sample are as Voltage 20 KV, working distance=10mm, spot size is sample area. Also high voltage mode is used. Material composition and dimensions of the microcantilever are observed. The SEM image by mounting the sample vertically is shown in Fig. 4.2.

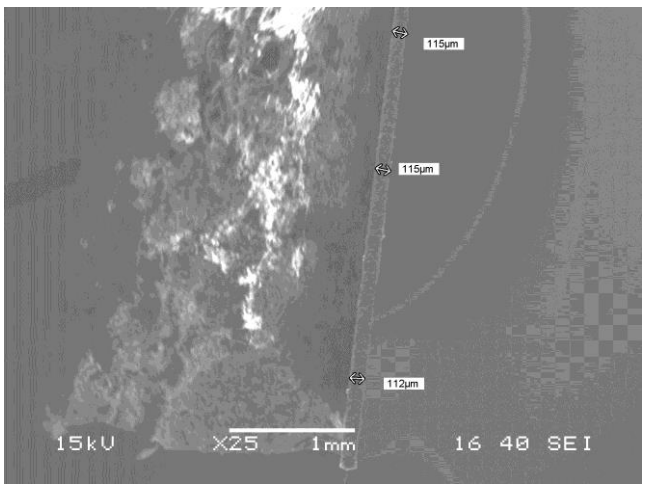

Fig 4.2 Measurement of height of microcantilever

Microscopic examination of the sample has given chemical composition and material data.

4.3 TEST BED DESCRIPTION

The experiment consists of the micro cantilever beam mounted on the rigid base, a mini-shaker unit (exciter) (5N), digital oscilloscope (Tektronics DPO 4034 Digital phosphor oscilloscope), a piezoelectric accerlometer, signal generator and power amplifier. The block diagram and connections made for vibration testing is as shown in following Fig. 4.3.

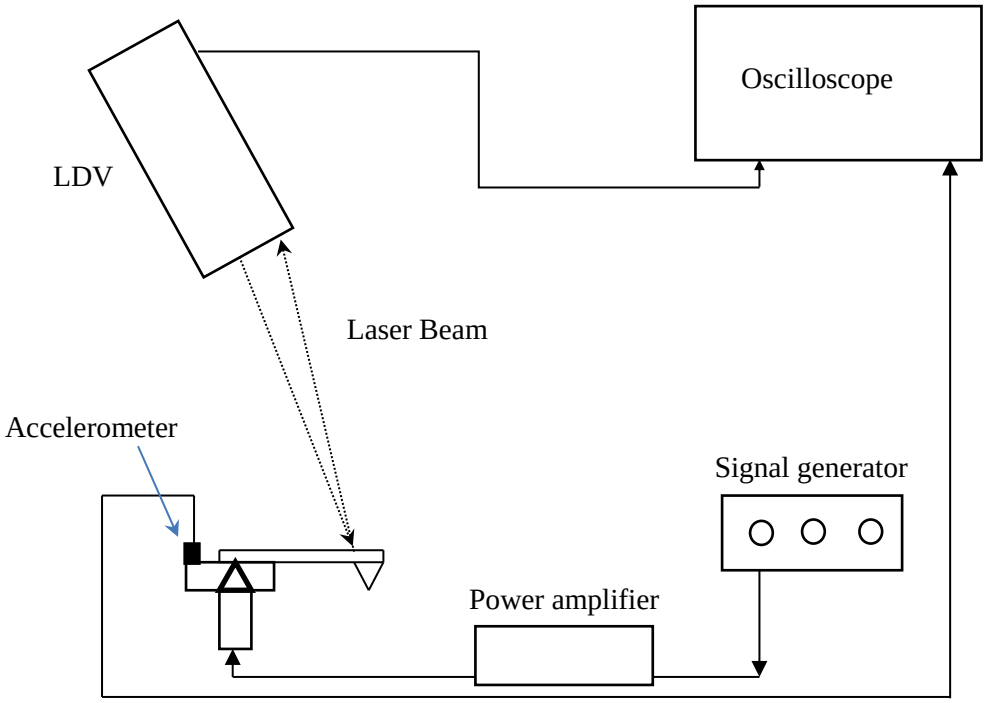

Fig 4.3. Block diagram for vibration testing.

Then microcantilever is fixed on the top edge base with the help of feviquick. Base is excited with the help of sinusoidal force from exciter. The amplitude of the force is maintained constant by using power amplifier continuously. An accelerometer mounted on the base of cantilever is used to measure the input waveform provided from signal generator and is connected to the oscilloscope at channel 1. To measure the vibrations of the cantilever, Laser Doppler Vibrometer (Ometron Vh 1000 D) is used. The laser beam is focused at the tip of the cantilever beam. The output of the laser beam is connected to the oscilloscope at channel 2. Fig.4.4 shows the physical set-up employed in the sweep-test experiment.

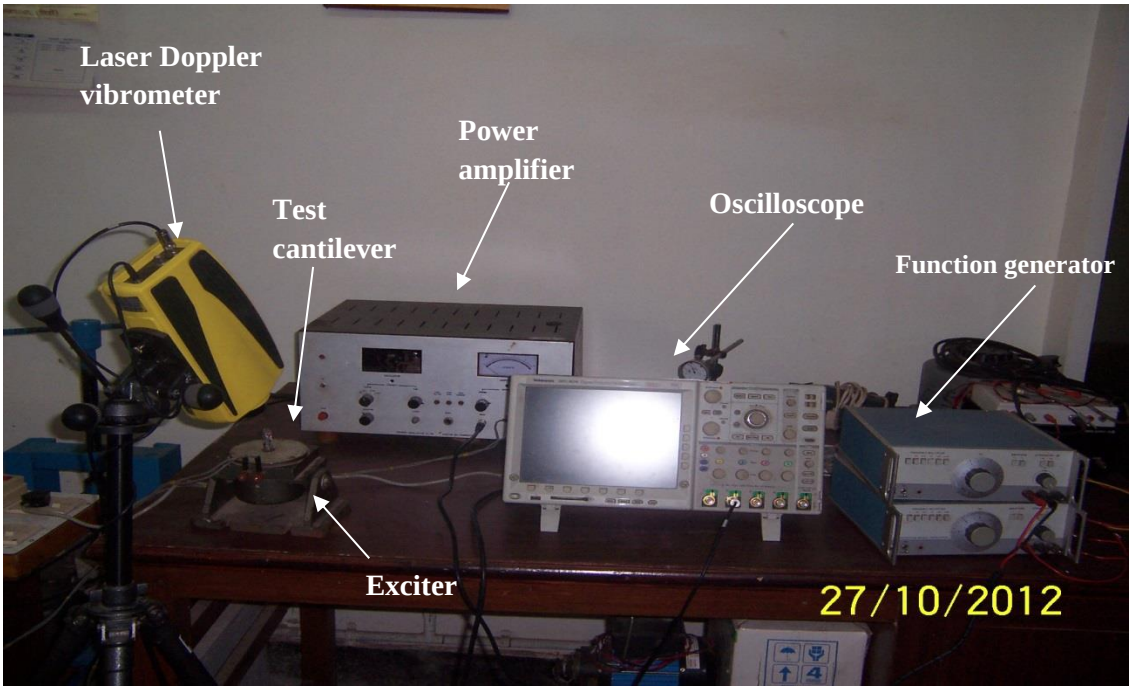

Fig 4.4 Experimental modal analysis on microcantilever

4.4 SINE SWEEP TESTING

Sine sweep vibration test is used to determine the certain natural frequencies of in structure. In sine sweep test, the output sensor (LDV) amplitudes are measured by increasing the excitation frequency at constant input amplitudes. The frequency is varied from 100Hz to10KHz in present case. Fig 4.5 shows screen shot of oscilloscope.

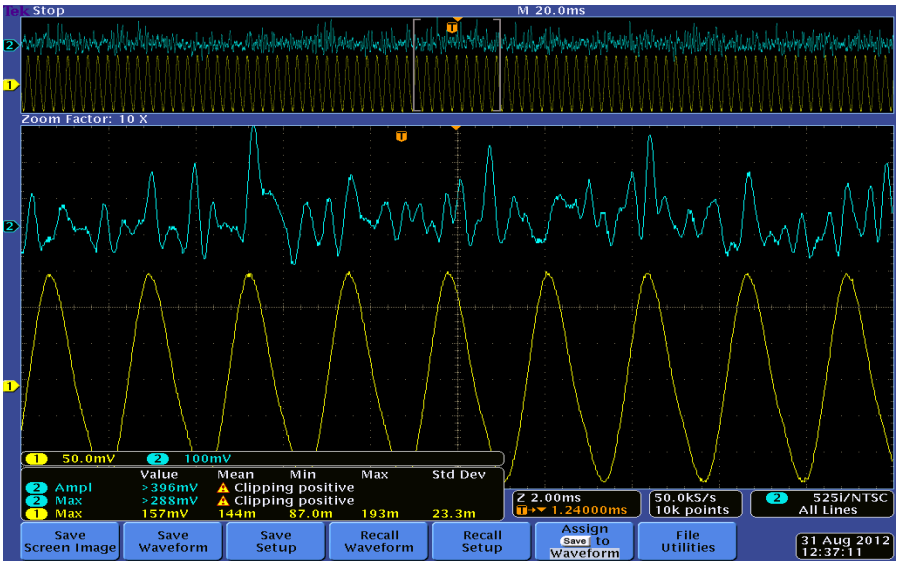

Fig 4.5 Screen shot of oscilloscope

4.5 EXPERIMENTAL RESULTS

The amplitudes of output sensor (LDV) are recorded at each frequency of input sinusoid. The output waveform is adjusted everytime till a sinusoidal signal is obtained. The output signal data is obtained both as a screenshot as well as an excel data file. Finally a graph is plotted between excitation frequency and output amplitudes from the specimen. Fig.4.6 shows the resultant frequency response drawn manually.

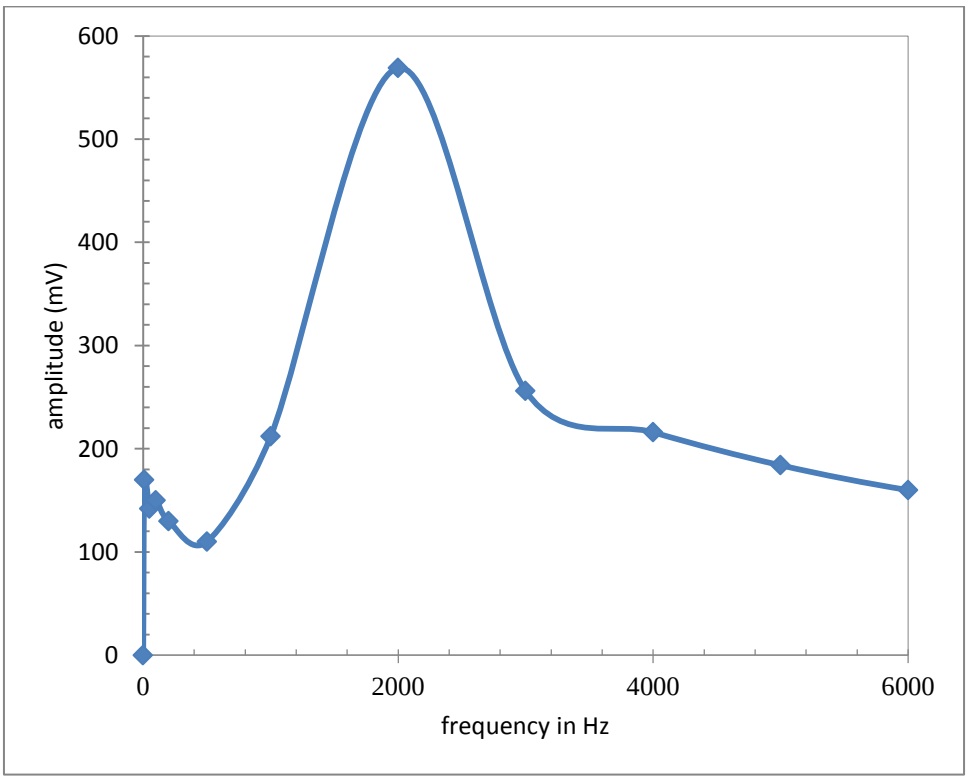

Fig.4.6 Experimentally obtained frequency response

By noting that the sample has no tip-mass, the results are compared with wellknown cantilever beam formula: $\omega_1 = \frac{3.5156}{\ell^2}\sqrt{\frac{EI}{\rho A}}$ rad/s. Experimentally measured resonance frequency is 2100Hz.

CHAPTER 5

5 CONCLUSIONS

In this work, analytical modeling of microcantilever beams with tipmass as application to atomic force microscopy has been presented. The effect of various forces like, nonlinear spring (beam nonlinarities)forces, interaction forces between tip and sample surface and hydrodynamic forces were observed on the dynamic stability of base excited cantilever. Interaction force was modeled by LJ potential force and DMT contact models, while system damping was idealized to be a combination of viscous and squeeze film damping (in liquids especially) and beam nonlinearity was modeled by cubic stiffness. All the studies were carried-out in tapping mode of operation. The analytical results were verified by lumped-parameter models and one mode approximated distributed-parameter models along with finite element analysis. A simple experiment analysis is conducted for obtaining the frequency response of the test specimen.

In overall sense, the objective of this study is to enhance the scanning ability of the system by proper design considerations of microcantilever beam. It is observed that the working performance of atomic force microscope in air is different from that in the liquid enviroments for the same microcantilever probe structure in terms of dynamic characteristics. There was a variation between the natural frequencies in air and liquid. Vibration amplitude and resonance frequency reduces as environment changes from the air to liquid. Frequency response in liquid environment is basically depends on two main parameters hydrodynamic and squeeze film forces and nonlinear tip sample interaction.

5.1 FUTURE SCOPE

As future scope of this work, the microcantilever beam dimensions are to be arrived for maximizing the quality factor and natural frequency. It requires actual microfabrication techniques to prepare the sample and test it in more accurate set-up like, scanning probe laser

Doppler vibrometers to get more inference. A user-interactive graphics user interface is to be developed to study the dynamic characteristics of the cantilever system operating both in liquids and air and an image processing software tool is to be linked up with the cantilever deflections to know the variations in scanning of samples. Further, a detailed study of stability issues of the cantilever is also an important task in future.

REFERENCES

[1] G. Binnig, C.F. Quate, and Ch. Gerber, "Atomic Force Microscope", *Physical Review Letters*, vol. 56, no. 9, pp. 930–933, 1986.

[2] A.Raman, J.Melcher and R.Tung, "Cantilever dynamics in atomic force microscopy", *Nanotoday*, vol.3, no.1-2, pp. 20-26, 2008.

[3] W. M. Zhang, G. Meng, J. B. Zhou and J. Y. Chen. "Nonlinear Dynamics and Chaos of Microcantilever-Based TM-AFMs with Squeeze Film Damping Effects", *Sensors*, vol. 9, pp. 3854-3874, 2009.

[4] A.F.Payam and M.Fathipour, "Modeling and Dynamic Analysis of Atomic Force Microscope based on Euler-Bernoulli beam theory", *Digest J.Nanomaterials and Biostructures*, vol. 4, pp. 565-578, 2009.

[5] M.H.Korayem, S.Zafari, A.Amanati, M.Damircheli and N.Ebrahimi, "Analysis and Control of micro-cantilever in dynamic mode AFM", *Int.J.Adv.Manuf Technol*, vol. 50, pp. 979-990, 2010.

[6] P. Brenetto and L. fortuna, S. Graziani and S. Strazzera, "A model of ionic polymer metal composites in underwater operations', *Smart materials and structures*, vol. 70, pp. 025-029, 2008

[7] Jin Woo Lee and Ryan Tung, Arvind Raman, Hartona sumali and Jonh P Sullivan,"Sqeeze film damping of flexible micro cantilever at low ambient pressures: theory and experiment", *Journal of micromechanics and microengineering*, vol. 19, pp 14, 2009.

[8] A.Sadeghi and H.Zohoor, "A fresh insight into the nonlinear vibration of double tapered atomic force microscope cantilevers by considering the Hertzian contact theory", *Proc. IMechE, Part:C, J. Mechanical Engineering Science*, vol. 225, pp. 233-241, 2010.

[9] Y.Zhang and K.D.Murphy, "Multi-modal analysis on the intermittent contact dynamics of atomic force microscope", *J.Sound and Vibration*, vol. 330, pp. 5569-5582, 2011.

[10] J. E. Sader, "Frequency response of cantilever beam immersed in viscous fluids with application to atomic force microscope", *Journal of applied physics*, vol. 84 pp. 64-76, 1998.

[11] C.A.J. Putman, K.O. Van der Werf, B.G. De Grooth, N.F. Van Hulst and J. Greve, "Tapping mode atomic force microscopy in liquid", *Appl. Phys. Lett.* vol. 64, pp. 2454, 1994..

[12] M. H. Korayem, H. Sharahi and A. H. Korayem, "Comparison of frequency response of atomic force microscopy cantilevers under tip sample interaction in air and liquids", *Scientia Iranica,* vol. 19, pp. 106-112, 2012.

[13] Y. Song, and B. Bhushan, "Finite-element vibration analysis of tapping mode atomic force microscopy in liquid", *Ultramicoscopy*, vol. 107, pp. 1095-1104, 2007.

[14] Y. Song and B. Bhushan, "Simulation of dynamic modes of atomic force microscopy using a 3D finite element model", *Ultramicroscopy,* 106, pp 847 – 873, 2006

[15] S. I. Lee, S. W. Howell, A. Raman, R. Reifenberger, "Nonlinear dynamic of microcantilever in tapping mode atomic force microscopy: A comparison between theory and experiment", *Physical review*, B 66, 115409, 2002.

[16] Awlad Hossain, Anamika Mishty and Ahsan Milan, "Numerical analysis for design optimization of microcantilever beams for measuring rheological properties of viscous fluid" *Finite element in Analysis and Design,* vol. 68, pp 1-9, 2013.

[17] C. Vancua, I. Dufour, S. Heinrich, F. Josse and A heirlemann, "Analysis of resonating microcantilever operating in liquid environment", *Sensors and Actuators, A,* vol. 141, pp. 43-51, 2008.

[18] Muramatsu H., Yamamoto Y., Shigeno M. and Shirakawabe Y., " Advanced tip design for liquid phase vibration mode atomic force microscopy", *Analytica chimiga acta 6II*, pp 233-238, 2008.

[19] Jones R. E. and Hart D. P.," Force interactions between substrates and SPM cantilevers immersed in fluids", *Tribology international,* vol. 38 pp. 355-361, 2008.

APPENDIX I

RUNGE KUTTA METHOD FOR TIME INTEGRATION

A forth order Runge's-Kutta Formula used for solving the first-oder differential equation $\frac{dy}{dx} = f(y,x)$ is

$$y = y_0 + \frac{1}{6}(k_1 + 2k_2 + 2k_3 + k_4)$$

Where

$$k_1 = hf(x_0, y_0),$$

$$k_2 = hf\left(x_0 + \frac{h}{2}, y_0 + \frac{k_1}{2}\right),$$

$$k_3 = hf\left(x_0 + \frac{h}{2}, y_0 + \frac{k_2}{2}\right),$$

$$k_4 = hf(x_0 + h, y_0 + k_3)$$

This is known as Runge-Kutta fourth oder method. The error in this formula is of the order h^4. This method has greater accuracy. This method is programmable using nested loops. In MATLAB, the values of *k, y* can be put into vectors to easily evaluate in matrix form. It can be extended for second order differential equations also by writing them as two first oder equations and solved them as simultaneous equations.

APPENDIX II

SYMBOLIC LOGIC TOOLBOX FOR SOLVING FREQUENCY EQUATION

Symbolic logic toolbox in MATLAB provides functions and interactive tool performing symbolic computations. It performs computations in terms of the symbols. Sometimes, this is of advantage such as in computation of definite differentials and integrals of various functions defined in symbols. In present work, the mode shape function is expressed in terms of the position variable (symbol) and the compuations are carried to solve and integrate the equations. For example to solve an equation: x2+2x+3=0 in symbolic logic toolbox, we write:

```
syms  x;

x=solve('x^2+2*x+3');
```

Similary int('x^2+2*x+3',0,5) is used to perform definite integration between the limits 0 to 5.

APPENDIX III

NEWTON RAPSON APPROACH FOR OBTAINING A SOLUTION TO FREQUENCY EQUATION

By this method, we get a closer approximation of the root of the equation if we already know its approximate root.

Let the equation be $f(x)=0$

Let its approximation root be a and better approximation root be $a+h$

Now we find *h*

$f(a+h)=0$ Approximately |as $a+h$, is the root of $f(x)=0$ (AIII.1)

By Taylor's theorem

$$f(a+h)=f(a)+hf'(a)+\frac{h^2}{2}f''(a)+\ldots$$

Or $$f(a+h)=f(a)+hf'(a) \quad \text{(AIII.2)}$$

Since *h* is veery small, we neglect h^2 the and higher power of *h*

From eq^n A1 and A2, we have

$$0=f(a)+hf'(a)$$

$$h=-\frac{f(a)}{f'(a)}$$

$$a+h=a-\frac{f(a)}{f'(a)}=a_1 \qquad \text{[First approximate root=}a\text{]}$$

Second approximate root $a_2=a_1-\frac{f(a_1)}{f'(a_1)}$

Similarly third approximation root $a_3=a_2-\frac{f(a_2)}{f'(a_2)}$

By repeating the operation we get a closer approximation of the root. "for" loop is used for repetetive iteration. So that it can be used for solving the frequency equation.

APPENDIX IV

SOLUTION FOR FREQUENCY EQUATION

Modal function is approximated in terms of frequency parameter β as:

$$\phi(x) = C_1 \cos \beta x + C_2 \sin \beta x + C_3 \cosh \beta x + C_4 \sinh \beta x$$

The constants C_1 to C_4 are obtained from following boundary conditions:

At $x = 0$, $\quad w(0,t) = 0 \quad \phi(0) = 0 \Rightarrow C_1 = -C_3$

At $x = 0$ $\quad w'(0,t) = 0 \quad \phi'(0) = 0 \Rightarrow C_2 = -C_4$

$$\therefore \ \phi(x) = C_1(\cos \beta x - \cosh \beta x) + C_2(\sin \beta x - \sinh \beta x)$$

Further at $x = L$: Bending moment: $EI \dfrac{d^2\phi}{dx^2} = K\phi''(L) = 0$

$$\Rightarrow C_1(-\cos \beta L - \cosh \beta L) + C_2(-\sin \beta L - \sinh \beta L) = 0 \qquad \text{(AIV.1)}$$

At $x = L$: Shear force: $EI \dfrac{d^3\phi}{dx^3} = K\phi'''(L) = m_e \dfrac{d^2w}{dt^2} - k_{ts} w(L,t)$

$$\Rightarrow \begin{aligned} &K\beta^3\left[C_1(\sin\beta L - \sinh\beta L) + C_2(-\cos\beta L - \cosh\beta L)\right]e^{j\omega t} \\ &= m_e\phi(L)(-\omega^2 \times e^{j\omega t}) - k_{ts}\phi(L)e^{j\omega t} \end{aligned}$$

$$\Rightarrow \begin{aligned} &K\beta^3\left[C_1(\sin\beta L - \sinh\beta L) + C_2(-\cos\beta L - \cosh\beta L)\right]e^{j\omega t} \\ &= -(m_e + k_{ts})\left[(C_1(\cos \beta L - \cosh \beta L) + C_2(\sin \beta L - \sinh \beta L)\right] \end{aligned}$$

$$\Rightarrow \begin{aligned} &\left[K\beta^3(\sin\beta L - \sinh\beta L) + (m_e + k_{ts})(\cos \beta L - \cosh \beta L)\right]C_1 \\ &-\left[K\beta^3(-\cos\beta L - \cosh\beta L) - (m_e + k_{ts})(\sin \beta L - \sinh \beta L)\right]C_2 = 0 \end{aligned} \qquad \text{(AIV.2)}$$

Eliminating C_1 and C_2 frm eqs.(AIV.1) and (AIV.2), we get the frequency equation in terms of β.

PAPER PUBISHED OUT OF THE THESIS

1. S. Manojkumar and prof. J. Srinivas, "Modelling of Atomic Force Microscope Probe with Base Motion", 9th Nanomechanical sensing conference at IIT Bombay, pp. 155-157, 2012

2. S. Manojkumar and prof. J. Srinivas, "Modeling of AFM Microcantilevers Operating in Tapping Mode" *International Journal of Applied Engineering Research,* vol. 7, No. 11, pp. 1347-1350, 2012.

3. S.Manojkumar and prof. J Srinivas, "Analysis of Cantilever beams in Liquid Media: A case study of a microcantilever", International journal of engineering sciences and inventions (IJESI) ISSN (Online): 2319 – 6734, ISSN (Print): 2319 – 6726, pp 57-61,2013